POLITECNICO
MILANO 1863

SCUOLA DI INGEGNERIA INDUSTRIALE
E DELL'INFORMAZIONE

Analytical and Experimental Investigation of Tapping Torque Prediction and Optimal Tap Core Diameter Determination

Tesi di Laurea Magistrale in
Mechanical Engineering - Ingegneria Meccanica

Author: **Jagan Sampath**

Student ID: 10934864
Advisor: Prof. Annoni Massimiliano Pietro Giovanni
Academic Year: 2025-26

Abstract

Thread tapping is a critical internal threading process in which tool failure often results from excessive torsional loading, chip congestion, or improper tool geometry selection. This study introduces an analytical and experimental framework to predict tapping torque and to determine the minimum safe core diameter of a tap necessary to prevent torsional fracture for a specific tool–workpiece combination.

Orthogonal cutting experiments were performed to determine the cutting and edge force coefficients for the selected material pair. These coefficients were subsequently converted into oblique cutting coefficients and integrated into a mechanistic tapping torque model that incorporates tool geometry parameters, including pitch, nominal diameter, pre-drill diameter, chamfer angle, chamfer length, and calibration length. The predicted maximum tapping torque was then applied in a torsional strength formulation, together with a safety factor, chip packing index, stress concentration factor, and material shear strength, to estimate the optimal tap core diameter.

Experimental tapping tests were conducted using multiple tap sizes, and the measured torque evolution, encompassing engagement, saturation, and disengagement stages, was compared with analytical predictions. The analytical model demonstrated strong agreement with experimental results, with only minor percentage deviations primarily attributed to friction variations and manual tapping conditions.

The proposed methodology enables reliable prediction of tapping torque and offers a systematic approach for selecting the minimum safe tap core diameter, thereby reducing tool breakage and enhancing the reliability of the tapping process.

Keywords: Tapping torque prediction, Tap core diameter design, Mechanistic modeling, Torsional failure of taps

Abstract in lingua italiana

La maschiatura è un processo critico di filettatura interna nel quale il cedimento dell'utensile è frequentemente causato da eccessivo carico torsionale, congestione del truciolo o selezione non appropriata della geometria dell'utensile. Il presente studio introduce un quadro analitico e sperimentale per la previsione della coppia di maschiatura e per la determinazione del diametro minimo sicuro del nocciolo del maschio necessario a prevenire la frattura torsionale per una specifica combinazione utensile–pezzo.

Sono state condotte prove di taglio ortogonale per determinare i coefficienti di forza di taglio e di spigolo relativi alla coppia di materiali selezionata. Tali coefficienti sono stati successivamente convertiti in coefficienti di taglio obliquo e integrati in un modello meccanicistico della coppia di maschiatura che incorpora i parametri geometrici dell'utensile, tra cui passo, diametro nominale, diametro di preforo, angolo di imbocco (chamfer), lunghezza di imbocco e lunghezza di calibrazione. La coppia massima di maschiatura prevista è stata quindi impiegata in una formulazione di resistenza torsionale, insieme a un fattore di sicurezza, un indice di impaccamento del truciolo, un fattore di concentrazione delle tensioni e la resistenza a taglio del materiale, al fine di stimare il diametro ottimale del nocciolo del maschio.

Sono state eseguite prove sperimentali di maschiatura utilizzando maschi di diverse dimensioni; l'evoluzione della coppia misurata, comprendente le fasi di ingaggio, saturazione e disimpegno, è stata confrontata con le previsioni analitiche. Il modello analitico ha mostrato una forte concordanza con i risultati sperimentali, con scostamenti percentuali contenuti, principalmente attribuibili a variazioni di attrito e alle condizioni di maschiatura manuale. La metodologia proposta consente una previsione affidabile della coppia di maschiatura e offre un approccio sistematico per la selezione del diametro minimo sicuro del nocciolo del maschio, riducendo così il rischio di rottura dell'utensile e migliorando l'affidabilità del processo di maschiatura.

Parole chiave: Previsione della coppia di maschiatura, Progettazione del diametro del nocciolo del maschi, Modellazione meccanicistica, Cedimento torsionale dei maschi

Contents

Introduction

0.1. Background and Motivation

Tapping is a widely employed manufacturing operation for producing internal threads in mechanical components, including housings, engine blocks, and machine parts. Although the process appears straightforward, tapping is mechanically complex because multiple cutting actions occur simultaneously on helical cutting edges under restricted chip-evacuation conditions.

Figure 1: Tapping operation

The torque generated during tapping determines tool life, thread accuracy, and overall process reliability. Excessive torque may cause tool breakage or thread form errors, whereas insufficient torque results in inadequate cutting engagement and defective threads. Consequently, the prediction and control of tapping torque are critical challenges in precision manufacturing.

Process parameters, including tool geometry (helix angle, rake angle, number of flutes, core diameter), cutting speed, feed rate, lubrication, and workpiece material, all influence tapping torque. Among these factors, tap geometry—particularly core diameter and predrill diameter—significantly affects torque behaviour and tool strength. A smaller core diameter increases torsional stress and the risk of fracture, while an oversized core diameter reduces chip space and may cause chip clogging and excessive torque.

Accurate analytical prediction of tapping torque facilitates process optimization and tool design, reducing dependence on costly experimental trials. While mechanistic and analytical cutting models have been successfully applied to orthogonal and oblique cutting processes [11], their adaptation to tapping, where chip thickness and cutting direction vary continuously, remains underdeveloped. Therefore, this research seeks to establish a generalized analytical–experimental framework for predicting tapping torque and determining optimal tap design parameters to ensure reliable operation.

0.2. Problem Statement

The existing literature offers several empirical and semi-analytical models for estimating tapping torque; however, these models are typically restricted to specific materials or tool geometries. A fundamental challenge is the absence of directly measurable cutting coefficients in the tapping configuration.

To address this limitation, the present study experimentally determines shear and edge force coefficients through orthogonal cutting tests, employing mechanistic approaches. These coefficients are then transformed into oblique cutting coefficients using geometric relationships based on helix and rake angles. The resulting coefficients are incorporated into an analytical torque model that accounts for the contribution of each active cutting edge.

A further challenge involves tap failure under torsional loading. Research on tool breakage and torsional strength [15] highlights the necessity of defining an optimal core diameter capable of withstanding maximum torque without surpassing the material's shear strength. Thus, a comprehensive analytical formulation that integrates torque prediction with torsional stress analysis is essential to ensure both the performance and safety of the tap.

Figure 2: Tapping tool breakage

0.3. Objectives of the Research

The research addresses the above problems through the following objectives:

1. To develop a predictive analytical model for estimating the maximum tapping torque based on cutting-mechanics principles.
    - The proposed model expresses torque as a function of shear and edge force coefficients, undeformed chip area, and tap geometry.
    - Orthogonal cutting experiments are conducted on C45 steel using M35 tool material to extract the necessary coefficients.
2. To validate the analytical models experimentally by measuring torque during actual tapping tests.
    - Real-time torque data are acquired using a piezoelectric torque sensor system.
    - A comparison between analytical predictions and measured torque is conducted to verify the predictive accuracy of the model.
3. To determine the optimal tap core diameter to prevent torsional failure during tapping operations.
    - Torsional stress relations are used to calculate the required core diameter, based on the maximum torque predicted by the analytical model.

Collectively, these objectives seek to establish a reliable correlation among process mechanics, tap design parameters, and observed torque behaviour.

0.4. Scope and Limitations

This study focuses on tapping C45 medium-carbon steel using M35 high-speed steel (HSS) taps. The scope encompasses both analytical modeling and experimental validation as outlined below:

- Analytical part:
    - Determination of shear and edge force coefficients from orthogonal cutting tests.
    - Transformation of orthogonal cutting coefficients to oblique cutting conditions.
    - Formulation of a predictive torque model incorporating geometrical and material parameters.

- Experimental part:
  - Measurement of cutting forces in orthogonal tests and torque in tapping using a piezoelectric transducer.
  - Evaluation of torsional failure and computation of the optimal tap diameter are performed based on maximum torque and stress analysis.

Limitations:

- The model assumes constant friction and a uniform chip load along the cutting edge [18].
- Tool wear, temperature variation, and lubrication effects are not explicitly incorporated.
- Experiments are limited to dry and controlled manual tapping conditions for a single material pair (C45–M35).

1 | Literature Review

Tapping is a complex machining process due to the tap's intricate geometry and the limited cutting environment inside the pre drilled hole. The tool's threaded profile creates significant contact with the workpiece, which increases cutting loads and makes the tool more susceptible to failure. Accurate torque prediction and tap design optimization depend on a comprehensive understanding of cutting mechanics and the interrelationships among tool geometry, material properties, and cutting parameters.

This chapter presents a comprehensive review of previous research on the analytical prediction of torque and the optimization of tap core diameter.

1. Fundamental studies on cutting-force modeling and coefficient identification,
2. Transformation from Orthogonal to Oblique cutting,
3. Analytical and mechanistic modeling of tapping torque,
4. Factors influencing torque and chip formation, and
5. Studies on torsional failure and tap design optimization.

The chapter concludes by identifying research gaps that motivate the present study.

1.1. Fundamentals of Cutting Mechanics

Accurate prediction of cutting forces and torque in machining relies on a thorough understanding of chip formation and the mechanics of material removal. Numerous studies have made substantial contributions to the development of cutting-force models.

Meier et al.[19] developed a generalized force and chip flow model for oblique cutting that accounts for variations in undeformed chip cross-sections. Their findings emphasize the geometric dependence of cutting forces in oblique cutting scenarios.

The mechanistic approach introduced by Bera et al.[3], and subsequently refined in turning and milling research, facilitates the determination of cutting coefficients through linear regression of specific forces with respect to uncut chip thickness. Similarly, Popović et al.

[25] and Popov & Dugin [24] investigated the relationship between uncut chip thickness and ploughing forces, demonstrating that total cutting forces can be represented as a linear combination of shear-dependent and edge-dependent terms. This principle underpins the orthogonal cutting tests conducted in the present study.

Yusuf Altintas, in Manufacturing Automation [1], systematized these concepts by presenting comprehensive models for chip formation, force decomposition, and coefficient identification. This framework distinctly separates the cutting and edge components of force and provides transformation equations between orthogonal and oblique cutting, which are essential for modeling helical cutting processes such as tapping.

Armarego and Chen [2] previously proposed predictive cutting models that integrate empirical and theoretical approaches to relate torque and thrust forces to tool geometry and cutting conditions. This has influenced the present research methodology, where experimentally derived orthogonal cutting coefficients serve as the basis for torque prediction.

1.2. Transformation from Orthogonal to Oblique Cutting

Transforming orthogonal cutting coefficients into oblique coefficients is essential for accurately modelling helical tools such as taps, drills, and end mills. Meier et al. [19] developed a comprehensive framework for predicting chip flow under various oblique conditions, and Lee and Altintas [14] derived transformation equations to convert orthogonal force coefficients into oblique components for milling tools.

These studies established the mathematical foundation for relating tangential, radial, and axial force components to fundamental cutting coefficients using trigonometric functions of rake and helix angles. The current research applies similar transformations to predict tangential and radial cutting coefficients relevant to tapping torque estimation.

1.3. Analytical and Mechanistic Models for Tapping

Initial investigations into tapping mechanics concentrated on empirical torque estimation. Henderer [12] and Lorenz [16] were among the first to examine cutting mechanics in tapping, offering experimental observations of torque variation as a function of tap geometry. Subsequently, Chen and Smith [7] expanded this work by modeling machine tapping with straight-flute taps, emphasizing the influence of rake angle, lead geometry, and hole characteristics on torque.

Armarego and Chen [2] enhanced the theoretical understanding of tapping forces by correlating torque prediction with cutting coefficients obtained from orthogonal tests, thereby establishing a foundation for mechanistic modeling approaches.

Tengyun Cao and Sutherland [6] further advanced the field by developing a mechanistic tapping model that integrated analytical relationships with experimental validation. Their research established the correlation among feed rate, spindle speed, and torque–thrust behavior.

Dogra et al. [9] utilized the mechanistic framework for fault detection in tapping, demonstrating that deviations in hole geometry significantly affect torque fluctuations. Oezkaya and Biermann [22] introduced the Geometrical Torque Prediction Method (GTPM), which automatically computes relative torque for different tap designs. In a subsequent study [21], they combined three-dimensional finite element method (3D FEM) simulations with the analytical approach, thereby narrowing the gap between empirical calibration and predictive modeling.

Pereira et al. [23] proposed an incremental torque model that calculates both torque and temperature distribution on a thread-by-thread basis. Gessner et al. [10] introduced a single-tooth analogy model, which enables direct measurement of each cutting tooth's contribution to the total torque.

Collectively, these studies have shaped the development of modern analytical tapping models. However, most rely on empirical calibration instead of using coefficients experimentally identified from fundamental cutting operations. This research directly addresses this gap.

1.4. Factors Affecting Tapping Torque and Chip Formation

Torque behavior during tapping depends on several parameters, such as friction, feed rate, helix angle, lubrication, and chip evacuation.

Saito et al. [28] investigated the effects of friction at the chip–tool interface and demonstrated its dominant role in determining chip shape and torque fluctuation. Min Wan et al. [29] emphasized the importance of feed error and indentation forces, showing that small deviations in feed per revolution can increase torque demand and induce indentation-related stress.

Demirel et al. [8] employed Finite Element Method (FEM) simulations to examine how

process parameters influence torque and thrust forces, confirming that cutting conditions and material properties directly affect these forces. Similarly, Bhowmick et al. [4] demonstrated that tool coatings and lubrication methods are critical for minimizing torque and extending tool life.

These findings indicate that a comprehensive torque model should account for geometric and kinematic parameters as well as frictional and material effects. In the present study, these factors are indirectly incorporated through experimentally identified coefficients and material properties.

1.5. Torsional Strength and Tap Failure Studies

Torsional overload-induced tool failure is a primary concern in tapping operations. Bodden et al. [5] conducted a failure analysis of high-speed steel taps and identified excessive torque and improper lubrication as principal contributors to fracture. Monka et al. [20] further investigated tap failure mechanisms, demonstrating that undersized core diameters increase torsional stress concentration and promote premature failure.

Henderer [12], Lorenz [16], and Chen & Smith [7] emphasized the relationship between torque magnitude and tap core diameter, indicating that appropriate core diameter design can significantly extend tool life.

These findings directly support another important objective of this thesis: to determine the optimal core diameter analytically using the torsional equation and the analytically predicted maximum torque. The stress concentration factor, identified experimentally in this research, establishes a critical connection between torque loading and material failure behaviour.

Oezkaya and Biermann [21] demonstrated that finite element method (FEM) analysis effectively captures stress concentration effects and validates analytical predictions of torque-induced failure.

1.6. Research Gap Identification

A comprehensive review of the literature reveals the following key research gaps:

1. Absence of a generalized analytical model capable of predicting tapping torque from first principles of cutting mechanics using measurable geometric and material parameters.

2. Limited transformation-based models connecting orthogonal cutting data to oblique tapping torque with experimentally validated coefficients.
3. Lack of analytical methods for tap core diameter optimization, even though torsional failure is well-documented.
4. Insufficient experimental–analytical validation, as most models depend on empirical fitting or simulation-only results [21].

To address these research gaps, this thesis:

- Develops a predictive analytical torque model based on experimentally identified shear and edge force coefficients from orthogonal cutting tests,
- Applies orthogonal-to-oblique transformation principles as established by Altintas [1] and related studies,
- Validates the model experimentally using a torque sensor and data acquisition system, and
- Determines the optimal tap core diameter analytically using torsional theory and experimental data to prevent tool failure.

This approach establishes a unified analytical–experimental framework for tapping torque prediction and tool design optimization.

2 | Analytical and Mechanistic Modeling of Tapping Torque

Predicting torque in tapping constitutes a complex mechanical problem that necessitates the integration of analytical geometry, material mechanics, and experimental calibration. Developing an accurate model for torque generated during thread formation facilitates process optimization, minimizes tool breakage, and supports the selection of optimal tap geometry for specific material combinations.

This chapter provides a comprehensive formulation of the analytical and mechanistic models employed to predict tapping torque.

The analysis is structured into five principal stages:

1. Formulation of cutting-force mechanics from fundamental chip-formation theory.
2. Derivation of analytical torque equations incorporating tool geometry and process parameters.
3. Experimental determination of cutting-force coefficients through orthogonal cutting tests.
4. Transformation of orthogonal coefficients to oblique coefficients, adapting them to the helical geometry of taps.
5. Integration of all components into a unified predictive torque-calculation framework.

2.1. Mechanics of Material Removal in Tapping

2.1.1. Nature of Chip Formation

During tapping, the cutting edges of the tap remove material from the pre-drilled hole, producing small helical chips that flow along the flutes of the tool. Unlike turning or milling operations, where the uncut chip thickness and width are generally constant, the

chip geometry in tapping changes along the chamfer section of the tap. This variation arises from the combined effect of the tool helix angle and the tapered chamfer geometry.

As the tap advances into the workpiece, each cutting edge progressively enters the material. Consequently, the chip thickness and the corresponding cutting load gradually increase along the chamfer region. When a cutting edge becomes fully engaged in the thread profile, the cutting conditions become relatively stable and the edge experiences nearly constant cutting forces.

This progressive engagement followed by steady cutting conditions results in a non-uniform distribution of load among the cutting edges, which influences the torque generation and tool life during the tapping process.

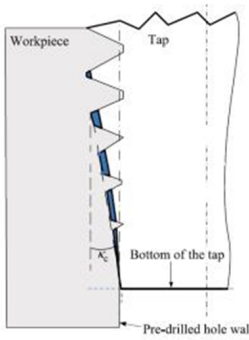

Figure 2.1: Schematic illustration of chip thickness

2.1.2. Decomposition of Cutting Forces

The elemental force components are:

- Tangential force dF_t: acts along the cutting velocity.
- Radial force dF_r: acts perpendicular to the tool axis and generates radial pressure.
- Axial force dF_a: acts parallel to the tool axis and contributes to the thrust load.

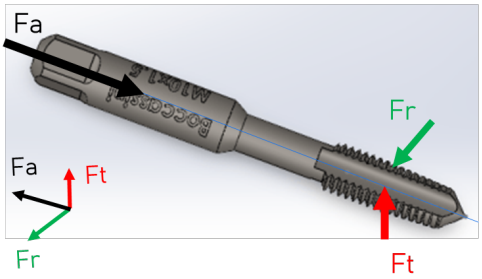

Figure 2.2: Elemental force components

Each force component arises from two physical mechanisms:

1. Shearing (cutting) component: associated with material separation.
2. Edge (ploughing) component: due to friction near the cutting edge.

According to the mechanistic force modeling approach [1], the elemental forces can be expressed as the sum of cutting and edge components:

$$dF_t = dF_{tc} + dF_{te}, \tag{2.1}$$

$$dF_r = dF_{rc} + dF_{re}, \tag{2.2}$$

$$dF_a = dF_{ac} + dF_{ae}. \tag{2.3}$$

2.2. Analytical Derivation of Torque

During the tapping operation, as the tap gradually enters the pre-drilled hole and engages the workpiece, each cutting edge (or tooth) experiences a complex system of forces arising from chip formation, friction, and tool–workpiece contact.

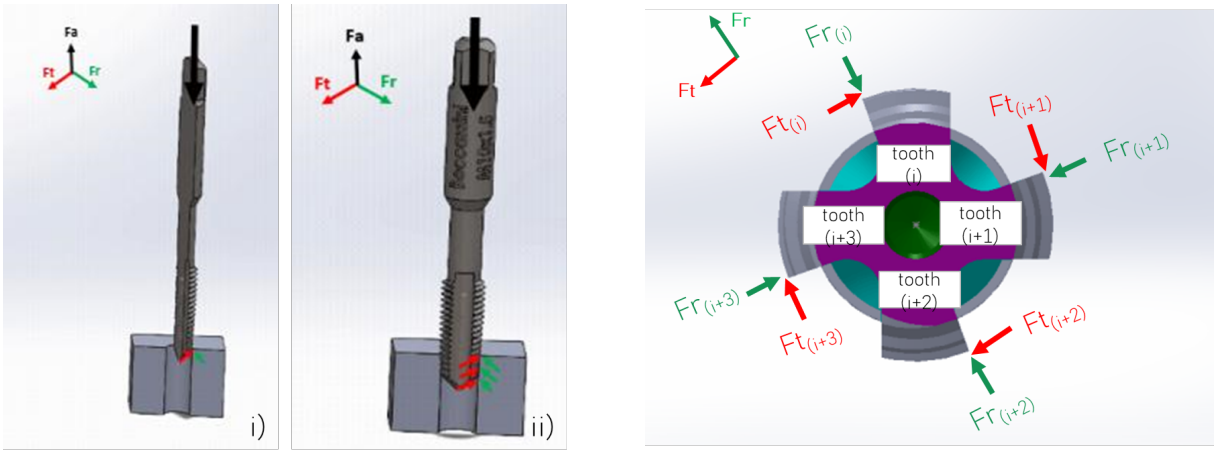

Figure 2.3: Force components acting on the teeth of the tap during the tapping process

The forces illustrated in the figure 2.3 represent the force components acting on the teeth of the tap during the tapping process. The tangential force $F_t(i)$ and radial force $F_r(i)$ shown in the right-hand schematic correspond to the force components acting on the each i-th tooth. These forces are applied at the teeth edge located at a specific axial position along the tap. As the tool advances into the workpiece, multiple teeth become engaged simultaneously. Therefore, the total forces and the resulting tapping torque are obtained by summing the contributions from all engaged teeth.

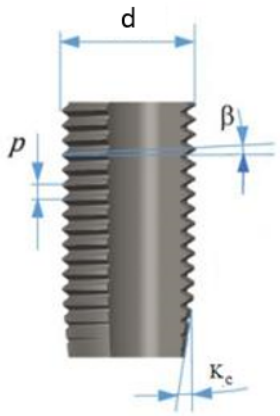

Figure 2.4: Tap nomenclature

2.2.1. Analytical Representation of tapping torque model

The fundamental analytical torque model, which was derived by Puzovic and Kokotovic [27], is used in this study,

$$T = \{[(K_{tc}A(i)) + (K_{te}L(i))]\cos\beta + [(K_{tc}A(i)) + (K_{re}L(i))]\sin\beta\}\, r \tag{2.4}$$

where,

A(i) = uncut chip cross-section area by a particular cutting tooth,

L(i) = cutting-edge contact length of a particular tooth.

K_{tc}, K_{te} and K_{re} - Force coefficients.

Equation 2.4 is used throughout the analytical prediction phase.

2.2.2. Geometric Determination of Chip Area and Edge Length

The magnitude of forces acting on a cutting edge depends on the instantaneous undeformed chip cross-section and the contact length between the tool and workpiece. Accurate geometric determination of the undeformed chip area ($A(i)$) and cutting-edge contact length ($L(i)$) is essential for reliable torque prediction.

Axial position of each cutting edge

When a tap enters the workpiece, each successive tooth engages the material at a slightly different axial position because of the thread pitch (p) and the number of flutes (z). The

chamfered region at the tip of the tap progressively increases the depth of engagement until the full thread profile is formed.

Let a be the radial depth of cut of the chamfer portion. The depth is calculated as the difference between the nominal diameter of the tap and the pre-drill hole diameter.

$$a = \frac{\text{Nominal diameter } (d) - \text{Pre-drill hole diameter } (d_p)}{2}$$

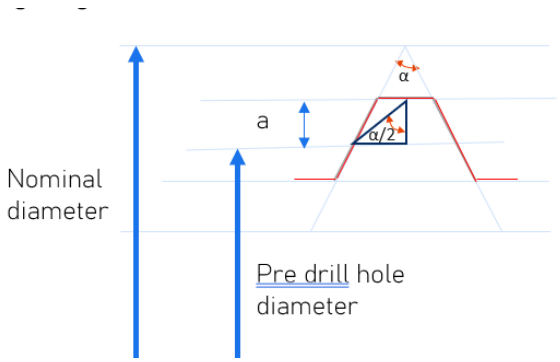

Figure 2.5: Depth of cut, illustration

The value a denotes the radial width of the chamfer portion, corresponding to the material removed radially to form the chamfer. This parameter is critical for defining chamfer geometry and ensuring proper fit and thread formation during tapping operations.

The axial position x_i of the i^{th} cutting edge (measured from the start of the chamfer) can be expressed as:

$$x_i = a * \tan\left(\frac{\alpha}{2}\right) + \frac{(i-1)p}{z} \tag{2.5}$$

where,

- α – thread profile angle (60°),
- p – thread pitch,
- z – number of flutes,
- i – tooth index.

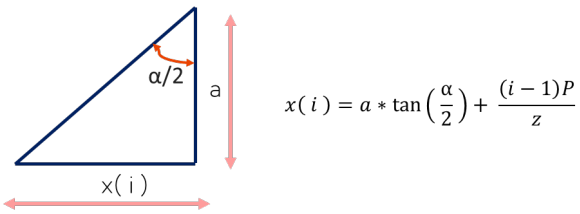

Figure 2.6: Axial position illustration

Since the cutting edges are uniformly distributed around the circumference of the tool, each tooth is angularly spaced by $2\pi/z$. Due to the helical geometry of the thread, this angular spacing produces an axial offset between consecutive teeth. The term $\frac{p}{z}$ therefore represents the axial shift between successive teeth along the helical cutting edge, which determines the relative axial position of each tooth during engagement.

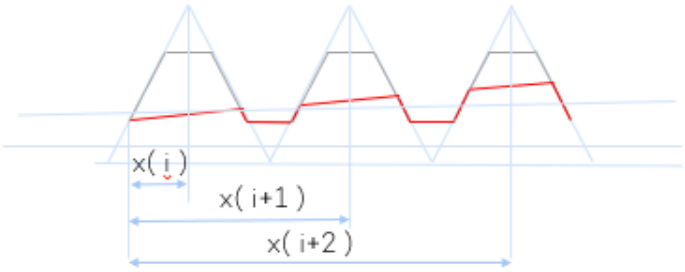

Figure 2.7: Axial position of each cutting edge

Uncut chip thickness for each tooth

For every cutting edge, the uncut chip thickness $H(i)$ corresponds to the instantaneous vertical height of material removed at that position.

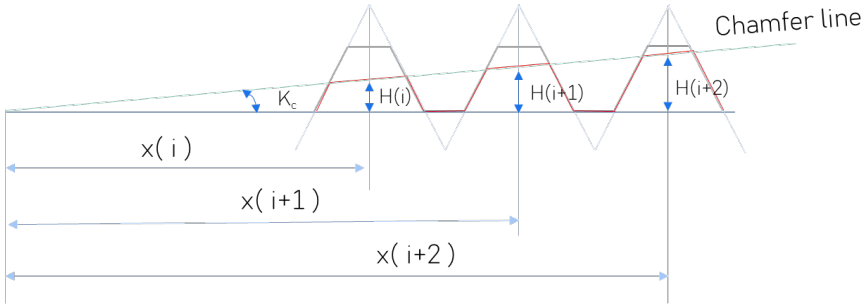

Figure 2.8: Uncut chip thickness of each cutting edge

Because the chamfer of the tap is ground at an inclination known as the chamfer angle (K_c), the uncut thickness increases linearly with the axial position:

$$H(i) = x(i) * \tan K_c \tag{2.6}$$

where K_c – chamfer angle of the tap, $x(i)$ - axial position of teeth.

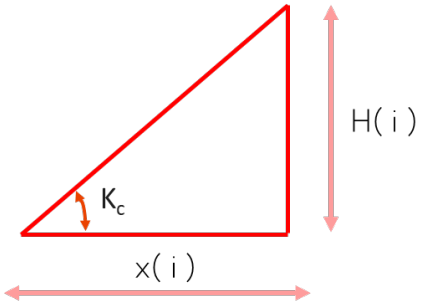

$$H(i) = x(i) * \tan(K_c)$$

Figure 2.9: Uncut chip thickness illustration

Equation 2.6 expresses how the engagement depth of successive teeth grows gradually along the chamfer section until the full thread depth is reached.

Undeformed chip area for each tooth

The material removed by one cutting edge can be approximated as a trapezoidal chip section, bounded by the uncut heights of the current and preceding teeth ($H(i)$ and $H(i-1)$).

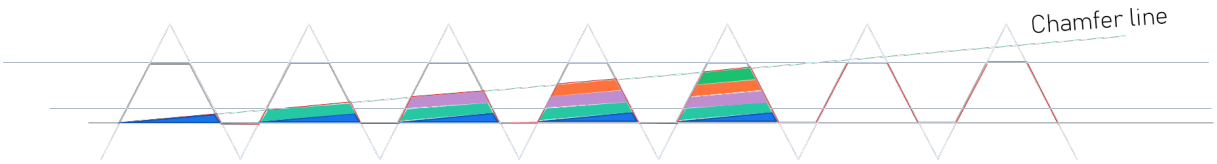

Figure 2.10: Undeformed chip area illustration

The undeformed chip area ($A(i)$) is therefore obtained by multiplying the effective width by the mean height of the trapezoid:

$$A(i) = b' \left(1 - \frac{H(i)}{2a}\right) (H(i) - H(i-1)) \tag{2.7}$$

Where, b' - maximum width of the undeformed chip, $H(i)$ - uncut heights/chip thickness of the current tooth and $H(i-1)$ - uncut heights/chip thickness of the preceding teeth.

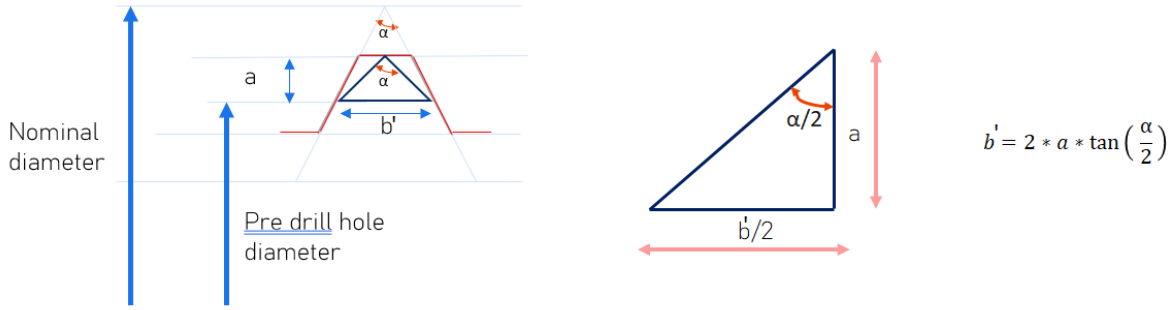

Figure 2.11: Undeformed chip maximum width illustration

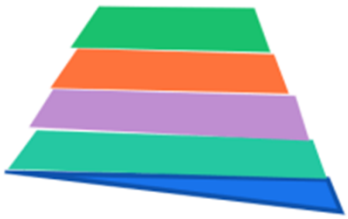

Figure 2.12: Undeformed chip area shape by each particular tooth

Equation 2.7 provides a simplified analytical expression for the instantaneous chip area removed by each active tooth in the cutting section.

This accounts for the geometric variation of chip thickness along the chamfer and is essential for force computation within the torque model.

Contact length of the cutting edge

The contact length ($L(i)$) represents the circumferential contact length of the cutting edge with the material at a given time.

The contact length differs between the cutting section and the calibration section of the tap.

- For the cutting (chamfer) section, the effective contact length varies with the progressive depth of cut and can be approximated as:

$$L(i) = b\left(1 - \frac{H(i)}{a}\right) + \frac{2a}{\cos\left(\frac{\alpha}{2}\right)} \tag{2.8}$$

where H_i is the local uncut height corresponding to the i^{th} tooth in the chamfer region.

- For the calibration section, where the full thread depth is constant, the contact length is determined purely by the flank geometry:

$$L(i) = \frac{2a}{\cos\left(\frac{\alpha}{2}\right)} \tag{2.9}$$

where a – full thread depth, α – thread profile angle.

Physical interpretation

The preceding derivations capture the geometric variation of engagement conditions along the chamfer. At the start of tapping, the first tooth removes only a small chip due to minimal uncut thickness, while subsequent teeth cut progressively thicker sections. Simultaneously, the contact length between the flank and the material increases until the full thread form is achieved. These geometric variations directly influence the distribution of cutting forces, and consequently, the torque and thrust developed during the process.

2.3. Mechanistic Modeling and Force Coefficients

Analytical expressions alone are insufficient to account for the effects of work-material microstructure, friction, and tool wear. Mechanistic modeling addresses this limitation by incorporating experimentally determined coefficients that quantify material-specific cutting behavior.

2.3.1. Kienzle–Altintas Linear Model

The mechanistic model expresses the elemental cutting force as a linear combination of the uncut chip area and the cutting edge length, as shown below:

$$dF_i = K_{ic}\, dA + K_{ie}\, dL \tag{3.3}$$

where K_{ic} and K_{ie} are the shear and edge coefficients for direction $i \in \{t, r, a\}$, corresponding to the tangential, radial, and axial force components, respectively.

The area-dependent term, defined by the shearing coefficient (K_{ic}), quantifies the force required for bulk plastic deformation and shearing of the workpiece material. In contrast,

the length-dependent term, defined by the edge coefficient (K_{ie}), accounts for non-shearing forces arising from friction, rubbing, and ploughing at the tool-workpiece interface, which are significantly affected by the finite tool edge radius. The Kienzle model is favored over earlier deterministic models, such as Merchant's, because it explicitly incorporates the cutting edge radius, a factor essential for accurately modeling forces at low chip loads encountered in finishing operations and in complex geometries such as threading.

Equation (3.3) forms the basis for computing cutting forces in most machining simulations [1].

2.3.2. Orthogonal Cutting — Principle and Analytical Significance

Accurate force and torque predictions in cutting models require reliable identification of fundamental cutting-force coefficients. These coefficients, which represent specific shear and edge forces, are intrinsic to the combination of work material, tool geometry, and cutting conditions. As they cannot be measured directly, they are typically determined through simplified and controlled cutting configurations, most commonly the orthogonal cutting test.

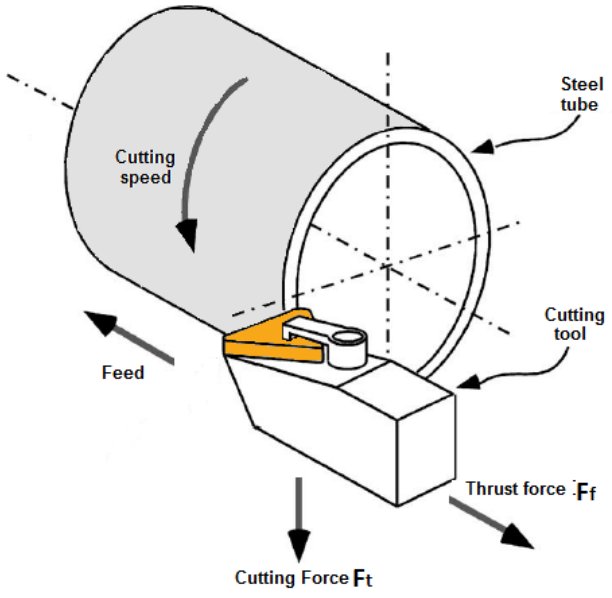

Figure 2.13: Orthogonal cutting illustration [17]

Purpose and Principle

The orthogonal cutting experiment provides a two-dimensional representation of the metal cutting process, where the cutting edge is set perpendicular to the direction of tool motion. This configuration eliminates the complexity introduced by a helical or oblique edge and allows the forces acting on the tool to be separated into two principal components:

- Tangential (cutting) force F_t, acting parallel to the cutting velocity.
- Feed (thrust) force F_f, acting perpendicular to the cutting direction.

Under these idealized conditions, the effects of tool geometry, chip thickness, and material deformation can be examined independently. This simplified arrangement allows for a direct correlation between uncut chip thickness (h) and the resulting forces per unit width of cut(b).

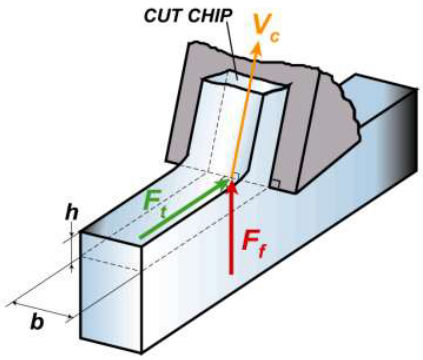

Figure 2.14: Orthogonal cutting force [1]

Relation to the Mechanistic Model

According to the mechanistic modeling approach (Altintas [1]; Bera et al. [3]), the specific cutting and edge forces in orthogonal cutting can be expressed linearly as:

$$\frac{F_t}{b} = K_{tc}\, h + K_{te}, \tag{2.10}$$

$$\frac{F_f}{b} = K_{rc}\, h + K_{re} \tag{2.11}$$

where:

- F_t, F_f are the tangential and feed forces (N),
- b is the depth of cut (mm),

- h is the uncut chip thickness (mm),
- K_{tc}, K_{rc} are the shear (cutting) coefficients in the tangential and feed directions,
- K_{te}, K_{re} are the edge (ploughing) coefficients in those directions.

The linear nature of these relationships indicates that as chip thickness increases, the cutting component becomes dominant, whereas the edge term accounts for frictional or ploughing effects that persist even at minimal chip thickness. Consequently, the slope and intercept of regression lines derived from force–thickness data correspond directly to the material-specific coefficients required for the analytical torque model.

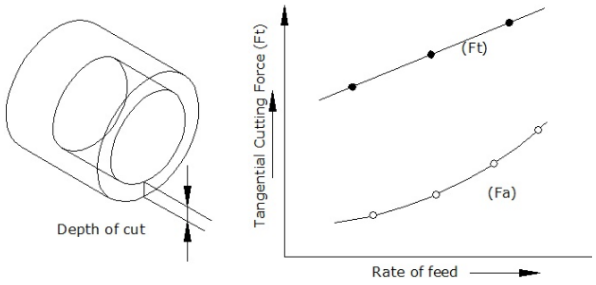

Figure 2.15: Effect of Feed vs Force

Extraction of Coefficients

From a conceptual standpoint, the procedure involves maintaining a constant depth of cut and tool geometry, while systematically varying the feed rate to obtain different chip thicknesses. The measured forces are normalized by the width of cut (b) to express them as specific cutting forces. By plotting $\frac{F_t}{b}$ and $\frac{F_f}{b}$ against h, two nearly linear trends are obtained. The slopes of these lines yield the shearing coefficients (K_{tc}, K_{rc}), whereas the intercepts provide the edge coefficients (K_{te}, K_{re}).

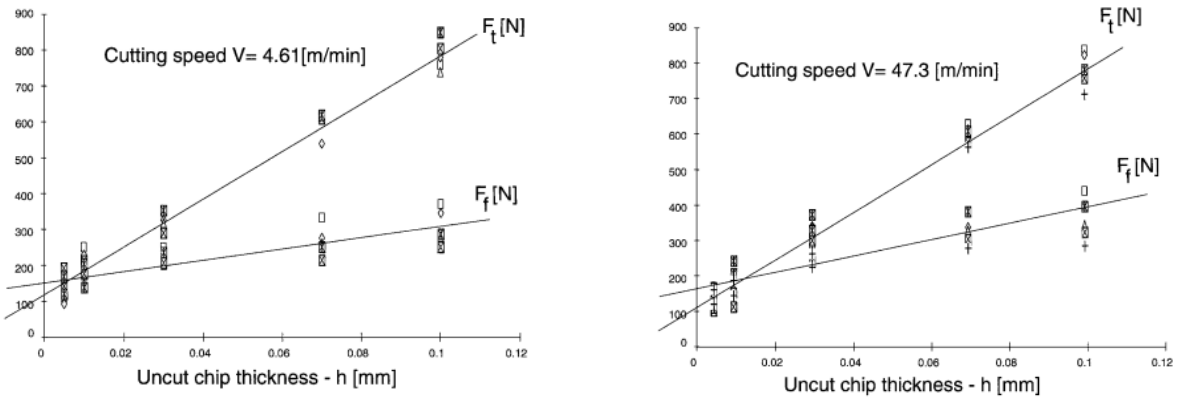

Figure 2.16: Orthogonal coefficients extraction

The above test image is taken from [1].

Connection to the Tapping Torque Model

The torque acting on the tap arises from the tangential and radial forces on the helical cutting edges. However, the coefficients in the analytical torque model — K_{tc}, K_{rc}, K_{te}, and K_{re} — are defined originally for orthogonal cutting. Therefore, the orthogonal test serves as the calibration step: it quantifies how the workpiece material resists shearing and edge deformation. These coefficients are then transformed mathematically using trigonometric relations involving the rake angle (γ) and helix angle (β) to obtain the corresponding oblique coefficients (K'_{tc}, K'_{te}, K'_{re}). These transformed parameters are finally substituted into the torque model:

$$T = \left\{ \left[(K'_{tc} A(i)) + (K'_{te} L(i)) \right] \cos\beta + \left[(K'_{tc} A(i)) + (K'_{re} L(i)) \right] \sin\beta \right\} * r \tag{2.12}$$

This logical progression establishes the orthogonal cutting experiment as the foundation of the analytical framework, rather than as an isolated laboratory test. It connects fundamental material behavior to predictive modeling of the tapping process, enabling accurate torque estimation and supporting tool design optimization.

2.3.3. Transformation from Orthogonal to Oblique Cutting

Tapping is inherently an oblique cutting process, as each tap tooth is inclined relative to the cutting velocity due to the helix geometry. Coefficients determined under orthogonal (two-dimensional) cutting conditions cannot be directly applied to oblique cutting predictions without a coordinate transformation. This section outlines the theoretical basis,

transformation formulae, and practical steps required to convert orthogonal shear and edge coefficients into oblique coefficients suitable for a helical tap.

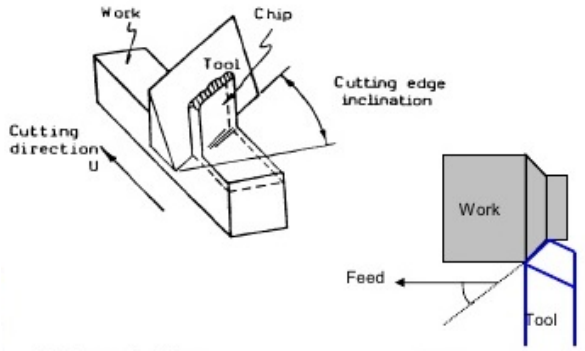

Figure 2.17: Oblique cutting illustration.png

The primary motivations for performing this transformation are as follows:

1. Orthogonal tests give reliable, easy-to-measure coefficients but for a 2-D geometry.
2. Oblique cutting changes the orientation of the shear plane and resolves forces differently into tangential, radial and axial directions.
3. A correct trigonometric transformation maps orthogonal coefficients, K_{ic} and K_{ie}, to an oblique set, K'_{ic} and K'_{ie}, used in the tapping torque model.

The transformation is based on kinematic geometry, including helix angle, rake angle, as well as a set of simplifying yet well-supported assumptions.

Governing assumptions

The transformation from orthogonal cutting coefficients (K_{ic}, K_{ie}) to oblique cutting coefficients (K'_{ic}, K'_{ie}) in mechanistic models, such as the tapping torque model, relies on several key assumptions to ensure analytical tractability and practical utility.

1. **Material Invariance:** Material properties (e.g., shear strength, friction characteristics) are identical for orthogonal and oblique cutting for the same tool–workpiece pair under similar cutting conditions. Thus, orthogonal coefficients reflect intrinsic material/tool interactions[26].
2. **Local Shear Angle Equivalence (Approximation):** The shear angle (ϕ') in the oblique cut is approximated by the shear angle (ϕ) measured in the orthogonal cut; small deviations are acceptable in first-order mechanistic models[1].

3. **Chip-Flow Angle Approximation:** The chip-flow angle η_c can be approximated by a function of the helix angle λ_s. A common first-order approximation is $\eta_c \approx \lambda_s$. This simplifies the geometry while retaining good accuracy for many taps[1].

Transformation of shearing coefficients

In orthogonal cutting, the shearing force arises from shear across a plane inclined at the shear angle. In oblique cutting, the shear plane rotates, causing the shearing component to project differently.

A commonly used set of transformation formulae (Altintas / Lee & Altintas derivations) for the shearing coefficients are:

$$K'_{tc} = K_{tc} \frac{\cos\eta_c \cos\lambda_s + \tan\gamma \sin\eta_c}{\cos(\eta_c - \lambda_s)} - K_{fc} \frac{\sin\eta_c \cos\alpha_n \cos\lambda_s - \sin\gamma \sin\lambda_s}{\cos(\eta_c - \lambda_s)} \tag{2.13}$$

(2.14)

- K_{tc} and K_{fc}: Orthogonal tangential and feed force coefficients.
- K'_{tc}: Oblique tangential force coefficients.
- η_c: Chip-flow angle.
- λ_s: Helix angle (or oblique angle).
- γ: Normal rake angle.

2.3.4. Transformation of edge (ploughing) coefficients

Edge or ploughing coefficients represent forces resulting from edge rounding, rubbing, and friction, acting along the tool face. Their transformation is comparatively straightforward because these forces act tangentially along the tool face rather than on a shear plane.

The typical transformation formulae for edge coefficients are:

$$K'_{te} = (K_{te} * \cos\lambda_s) - (K_{fe} * \sin\lambda_s * \sin\gamma) \tag{2.15}$$

$$K'_{re} = (K_{te} * \sin\lambda_s \sin\eta_c) + (K_{fe} * \cos\gamma * \cos\eta_c) \tag{2.16}$$

2.4. Total Torque Prediction

For a tap with N active cutting edge, the total torque is:

$$T_{\text{total}} = r * \sum_{i=1}^{N} \{[(K'_{tc}A(i)) + (K'_{te}L(i))]\cos\beta + [(K'_{tc}A(i)) + (K'_{re}L(i))]\sin\beta\} \quad (2.17)$$

2.5. Summary

This chapter provided a comprehensive derivation of the analytical and mechanistic models employed for tapping torque prediction.

Key outcomes include:

1. Development of the analytical torque equation linking torque to cutting coefficients, chip area, and tap geometry.
2. Definition of a procedure for the experimental determination of shear and edge coefficients from orthogonal cutting tests using regression analysis.
3. Mathematical transformation of coefficients from orthogonal to oblique coordinates suitable for helical flutes.
4. Integration of differential forces to predict total torque.

These models form the basis for the experimental validation and optimal core-diameter analysis presented in the following chapters.

3 | Experimental Methodology

This chapter outlines the experimental methodology implemented to support the analytical modeling of tapping torque presented in the previous chapter. The experimental work was structured in two distinct phases, each addressing a specific objective within the research framework:

1. **Orthogonal cutting experiments**, were conducted to identify the cutting and edge force coefficients necessary for calibrating the mechanistic force model.
2. **Tapping experiments**,were performed to measure the tapping torque and validate the analytical torque prediction model.

3.1. Orthogonal Cutting Experiments (Calibration)

3.1.1. Objective

This experimental methodology was implemented to determine the cutting force coefficients necessary for analytical prediction of tapping torque. Due to the complexity of directly measuring cutting force coefficients during tapping, which involves a multi-tooth and oblique cutting process, an equivalent orthogonal cutting approach was utilized.

Orthogonal cutting experiments were conducted on C45 steel using a high-speed steel (HSS) M35 cutting tool manufactured to match the material of the actual tapping tool. The measured cutting forces were used to identify tangential cutting and edge force coefficients through a mechanistic modeling approach. These coefficients were subsequently transformed into radial force coefficients using tool geometry parameters, enabling their use in the tapping torque prediction model developed in the previous chapter.

The experimental procedure systematically varied the feed rate while maintaining constant cutting velocity and depth of cut. Force data were acquired indirectly via spindle motor torque signals from the CNC lathe control system, converted to cutting forces, and analyzed during the steady-state cutting regime.

3.1.2. Workpiece Material and Geometry

Workpiece Material: C45 Steel

C45 medium-carbon steel was chosen as the workpiece material for the orthogonal cutting experiments. This material is widely utilized in mechanical components and frequently subjected to tapping operations in industrial applications.

Workpiece Geometry

A tubular workpiece geometry was employed to achieve orthogonal cutting conditions while maintaining a constant engagement width. The workpiece dimensions were as follows:

- Outer diameter (OD): 64 mm
- Inner diameter (ID): 61 mm
- Wall thickness: 1.5 mm

Figure 3.1: C45 - Workpiece

This tubular geometry ensured a uniform cutting width during turning and minimized force variations resulting from changes in chip load, compared to the solid shaft geometry. The thin-walled tubular configuration enabled the cutting process to closely approximate ideal orthogonal cutting conditions, with the cutting edge perpendicular to the cutting velocity and chip flow occurring in a single plane.

3.1.3. Cutting Tool Material and Geometry

Tool Material: M30 High-Speed Steel

The cutting tool for the orthogonal cutting experiments was manufactured from M35 medium-carbon high-speed steel and heat treated to a hardness of 64–66 HRC. This

material and hardness were selected to closely replicate the properties of the actual tapping tool used in subsequent stages of the study. Employing the same tool material and heat treatment condition ensures consistency between the experimentally determined force coefficients and their application in the tapping torque model.

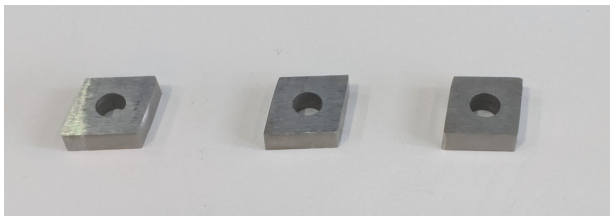

Figure 3.2: M35 HSS - Tool

The heat-treated M35 HSS offers enhanced wear resistance and maintains cutting edge integrity at the selected cutting speed, enabling stable and repeatable force measurements across multiple tests.

Tool Geometry and Insert Design

The cutting tool geometry was designed in accordance with the CNMG120404 insert standard. The tool was custom-manufactured to replicate the rake angle, clearance angle, and edge geometry of the standard insert, while ensuring compatibility with the CNC lathe tool holder. (Used CNC lathe model - CMZ Machinery (TD-20-TY-800) and Tool holder model - Walter (C4-DCLNR-27050-12))

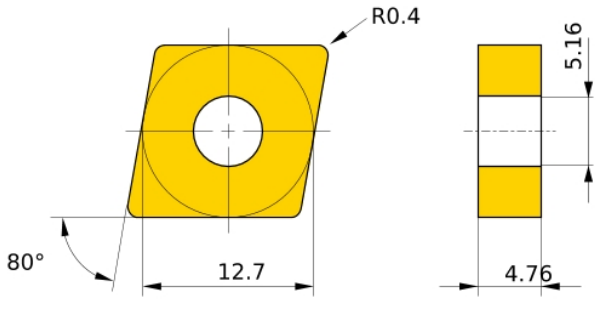

(a) CNMG120404 Insert design parameters

(b) Insert mounted in tool holder

Figure 3.3: M35 HSS Tool in Tool holder

3.1.4. Machine Tool and Measurement System

CNC Lathe and Control System

All orthogonal cutting experiments were conducted on a CNC lathe equipped with a FANUC(i-series) control system. The machine enabled precise control of spindle speed, feed rate, and depth of cut, ensuring stable and repeatable cutting conditions throughout the experiments.

The spindle drive system of the CNC lathe provides real-time torque feedback as a percentage of the maximum available spindle torque. This signal served as the primary measurement for force estimation.

Figure 3.4: CNC lathe machine with FUNUC (i-series) control system

Force Measurement via Spindle Motor Torque

Direct force measurement with a dynamometer was not utilized in this study. Instead, cutting forces were indirectly determined using the spindle motor torque signal obtained from the CNC controller. This approach enables the estimation of cutting forces without the need for additional external sensors or modifications to the machine tool setup. Moreover, the use of internal machine signals is consistent with the principles of Industry 4.0, which promote the integration of digital data from machine tools for process monitoring and analysis. Such sensorless monitoring strategies allow cost-effective implementation of machining diagnostics and facilitate the development of smart manufacturing systems.

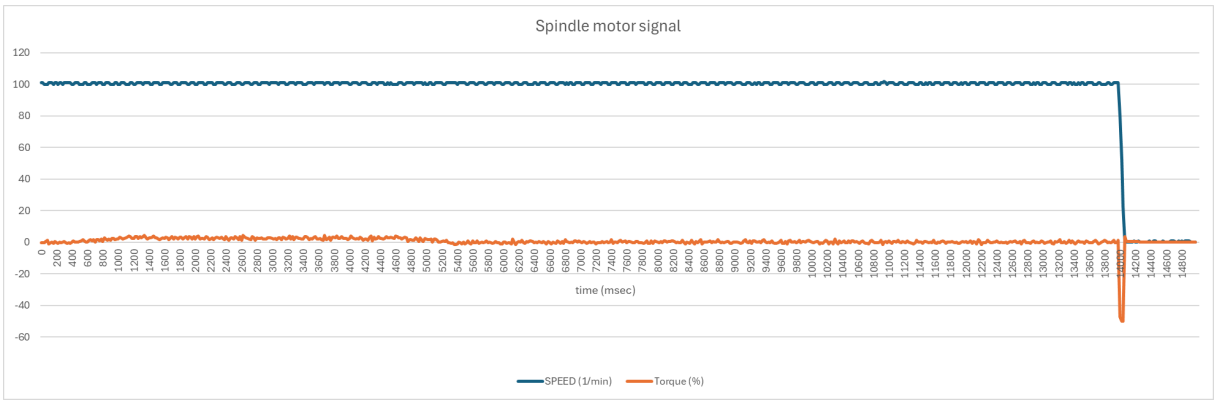

Figure 3.5: Spindle motor signal - FUNUC controller

The spindle torque signal was recorded as a percentage of the maximum spindle torque capacity. This value was converted to actual torque using the machine's rated constant torque(286 Nm).

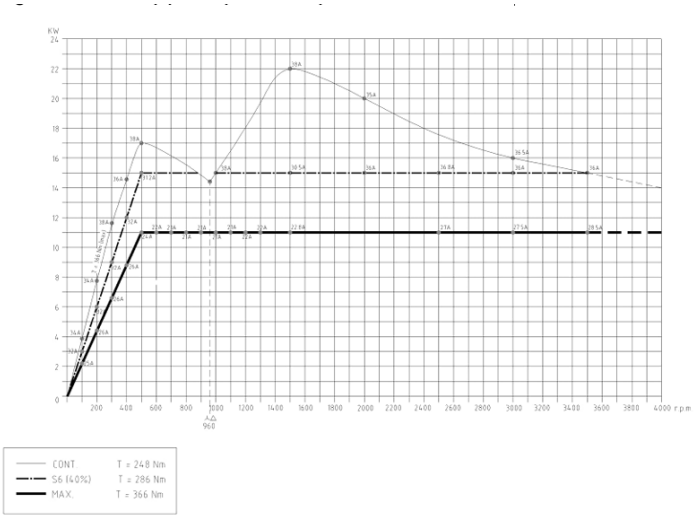

Figure 3.6: Power-Speed characteristic curve of motor

The tangential cutting force was subsequently calculated from the measured torque using the following relation:

$$F_t = \frac{T}{r} \tag{3.1}$$

where: F_t is the tangential cutting force, T is the spindle torque and r is the effective cutting radius.

This method enables reliable estimation of cutting forces during steady-state cutting, particularly when relative force trends and averaged values are required.

3.1.5. Experimental Cutting Conditions

Cutting Parameters

The orthogonal cutting experiments were conducted under controlled and repeatable conditions to ensure reliable force measurements. The selected cutting parameters are summarized as follows:

- Cutting velocity: 20 m/min (recommended for C45 steel from [13]
- Depth of cut: 1.5 mm
- Spindle speeds: 100 rpm and 150 rpm ($Speed = \frac{CuttingVelocity \times 1000}{\pi \times OuterDiameter}$)
- Feed/revolution: 0.15, 0.20, 0.30, and 0.45 mm/rev

The cutting velocity was maintained constant by adjusting the spindle speed according to the workpiece diameter. To assess repeatability, experiments were repeated twice at a spindle speed of 100 rpm and once at 150 rpm. This approach verified that the experimentally determined force coefficients remained consistent at identical cutting velocities, confirming the robustness of the force model.

Experimental Matrix

The experimental matrix was designed to investigate the effect of feed rate on cutting forces and to assess repeatability at different spindle speeds. At 100 rpm, feed rates of 0.15, 0.20, 0.30, and 0.45 mm/rev were tested, with each condition repeated twice. At 150 rpm, feed rates of 0.15, 0.20, and 0.30 mm/rev were tested once.

Spindle Speed (rpm)	Feed value (mm/rev)	Repetitions
100	0.15	2
100	0.20	2
100	0.30	2
100	0.45	2
150	0.15	1
150	0.20	1
150	0.30	1

Table 3.1: Experimental matrix for evaluating feed rate effects on cutting forces

This experimental arrangement enabled systematic evaluation of feed rate effects on cutting forces. The repeated trials at 100 rpm verified the consistency and robustness of the force coefficient extraction methodology(refer to Appendix A).

3.1.6. Data Processing and Coefficient Identification

Steady-State Force Extraction

During each orthogonal cutting test, the measured force signal initially increased as the cutting insert engaged the workpiece, due to the transient increase in chip thickness before the steady removal of material. Once the chip thickness stabilized at its nominal value corresponding to the prescribed depth of cut, the force signal reached a steady-state region, reflecting uniform orthogonal cutting conditions. Upon completion of the cut, the force signal decreased as the insert disengaged from the workpiece.

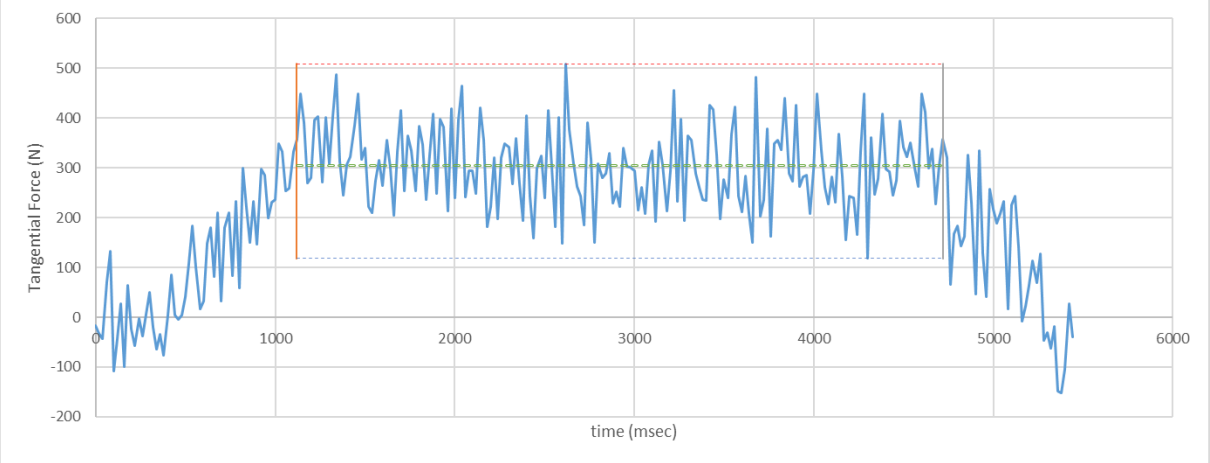

Figure 3.7: Average force extraction at steady state

To obtain representative force values, the tangential force was averaged over the steady-state region. The initial and final transient portions of the signal were excluded, as they represent partial engagement and disengagement and do not reflect steady orthogonal cutting mechanics. This approach minimizes the influence of transient effects and provides a reliable estimate of the true cutting force for each feed rate(refer to Appendix A).

Calculation of Uncut Chip Thickness

The uncut chip thickness, h, for orthogonal cutting was calculated directly from the feed rate per revolution. Because the cutting width remained constant due to the tubular workpiece geometry, variations in measured cutting forces were primarily attributed to changes in uncut chip thickness.

Linear Regression and Coefficient Extraction

From the orthogonal cutting experiments conducted with the selected tool–workpiece combination, the cutting force coefficients were identified using linear regression of the tangential force per chip width (F_t/b) as a function of uncut chip thickness (h).

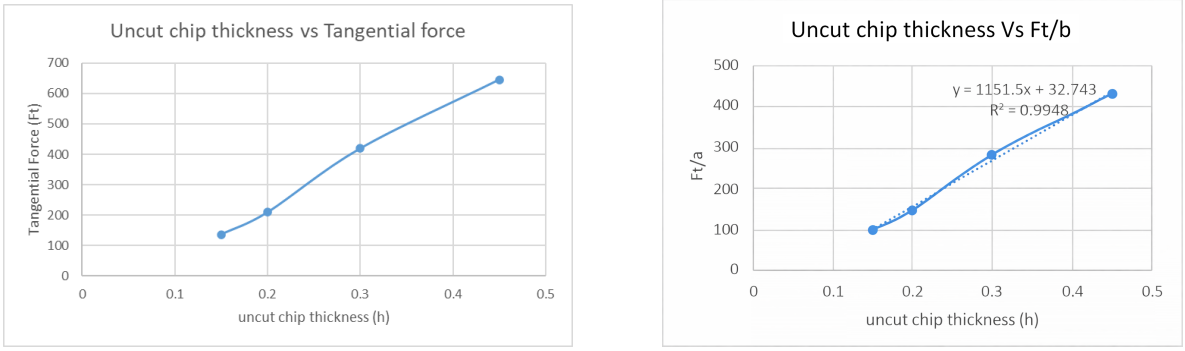

(a) h vs Ft

(b) h vs Ft/b

Figure 3.8: Extracting force coefficients

The relationship between tangential force and chip thickness in orthogonal cutting can be expressed as,

$$\frac{F_t}{b} = K_{tc}\, h + K_{te} \tag{3.2}$$

Based on the experimental results and linear fitting of the steady-state cutting data, the following coefficients were obtained for the investigated tool–workpiece pair:

$$K_{tc} = 1151.5 \text{ N/mm}^2$$
$$K_{te} = 32.7 \text{ N/mm}$$

The high coefficient of determination ($R^2 = 0.9948$) confirms the linear relationship between cutting force and uncut chip thickness, validating the applicability of the mechanistic force model for this material and tool combination.

Because tapping is an oblique cutting process, the orthogonal cutting coefficients must be transformed into their corresponding oblique cutting coefficients before implementation in the tapping torque prediction model.

Using the established orthogonal-to-oblique transformation methodology, the required oblique force coefficients were determined from the identified orthogonal coefficients. These transformed coefficients were then used in the analytical tapping torque model to predict torque.

3.2. Tapping Experiments (Validation)

3.2.1. Objective

Tapping experiments were performed to measure the torque generated during actual tapping operations and to validate the analytical torque prediction model, which was developed using force coefficients derived from orthogonal cutting experiments.

In contrast to orthogonal cutting, tapping involves multi-tooth engagement, oblique cutting conditions, and complex chip evacuation. Consequently, direct experimental validation is necessary to assess the predictive accuracy and practical applicability of the analytical model.

3.2.2. Workpiece Material and Preparation

Tapping experiments utilized workpieces fabricated from the same C45 steel as used in the orthogonal cutting experiments, thereby ensuring material consistency between model calibration and validation stages.

(a) CAD design (b) Real Workpiece

Figure 3.9: C45 tapping experimental workpiece

The workpieces were fabricated as solid cylindrical blocks with a thickness of 20 mm, to enable secure mounting to the torque sensor(Kistler 9369A) for tapping torque measurements. A pre-drilled central hole was prepared in each workpiece, with the diameter selected according to standard tapping recommendations for the corresponding tap sizes.

This configuration provided proper alignment with the torque measurement system, stable clamping during tapping, and repeatable experimental conditions, thereby enhancing the accuracy and reliability of the measured tapping torque data.

3.2.3. Selection of Tapping Tools for Experimental Validation

Tapping experiments employed taps manufactured from M35 high-speed steel (HSS), consistent with the tool material used in the orthogonal cutting experiments. This approach ensured material consistency between force coefficient identification and tapping torque validation.

A set of commercially available taps with varying sizes and geometric characteristics was selected to experimentally validate the analytically predicted tapping torque.

Tap	**Pitch** (mm)	**Pre-drill dia (mm)**	**Chamfer angle (°)**	**Chamfer length (mm)**	**Calibration length (mm)**
M5 × 0.8	0.8	4.2	19	$3 \times Pitch$	12.6
M6 × 1	1.0	5.0	5	$7 \times Pitch$	8.0
M8 × 1.25	1.25	6.8	8	$5 \times Pitch$	8.75
M10 × 1.5	1.5	8.5	19	$3 \times Pitch$	12
M12 × 1.75	1.75	10.5	8	$5 \times Pitch$	6.25

Table 3.2: Geometric parameters of taps used for experimental validation

Experiments utilized taps of sizes M5 × 0.8, M6 × 1, M8 × 1.25, M10 × 1.5, and M12 × 1.75, all manufactured from M35 high-speed steel (HSS) and featuring three flutes. The corresponding pre-drilled hole diameters were chosen according to standard tapping recommendations for each thread size.

The taps varied in key geometric parameters, including pitch, chamfer angle, chamfer length, and calibration length, while maintaining a constant rake angle of 12° and a thread profile angle of 60°. This design enabled systematic assessment of the influence of tap size and chamfer geometry on torque development.

3.2.4. Torque Measurement Hardware and Instrumentation

The torque generated during manual tapping was measured using a high-precision system comprising a Kistler 9369A torque sensor, a Kistler Type 5015 charge amplifier, and a National Instruments NI 9234 data acquisition (DAQ) module

The Kistler 9369A rotary torque sensor measured the torque transmitted during manual tapping. The sensor was rigidly mounted on the machine table, and the workpiece was firmly attached to the sensor. This arrangement ensured concentric alignment between the tap and the torque sensor axis, minimizing measurement errors from eccentric loading

or bending moments.

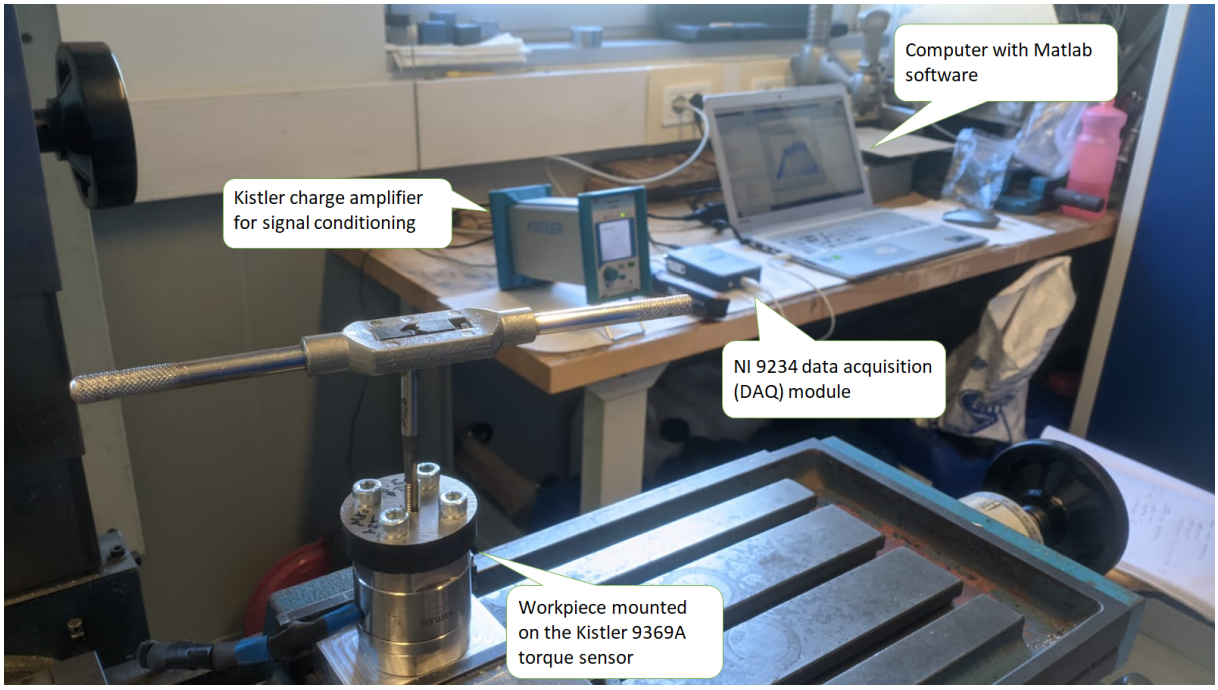

Figure 3.10: Tapping experimental setup

The overall experimental setup, illustrated in Figure 3.10, consisted of the following components:

- Workpiece mounted on the Kistler 9369A torque sensor
- Kistler charge amplifier for signal conditioning
- National Instruments NI 9234 data acquisition (DAQ) module
- Computer with Matlab software for real-time data acquisition and monitoring

This setup facilitated precise measurement of the torque generated during manual tapping.

The Kistler 9369A torque sensor was chosen for its high sensitivity and suitability for measuring the low to medium torque levels typically encountered during tapping operations. The sensor converts applied mechanical torque into a proportional electrical charge signal.

Because the torque sensor output is charge-based, a Kistler Type 5015 charge amplifier was used to condition the signal. The amplifier converts the charge output into a voltage signal with calibrated sensitivity, enabling compatibility with standard voltage-based data acquisition systems.

(a) Kistler 9369A Torque sensor (b) Kistler charge amplifier (c) NI 9234 DAQ module

Figure 3.11: Devices used in tapping experiment

The conditioned voltage signal was acquired using a National Instruments NI 9234 DAQ module, a 4-channel, 24-bit resolution device with an input range of ±5 V. The high resolution of the NI 9234 ensured accurate digitization of small torque variations during the tapping process.

The DAQ module was connected to a laptop computer, where MATLAB was employed for real-time data acquisition, signal processing, and post-analysis.

3.2.5. Data Acquisition Procedure

Data acquisition was conducted using MATLAB's Data Acquisition Toolbox, which enabled direct communication with the National Instruments hardware.

The torque signal was sampled at 51.2 kHz, a power-of-two–based rate ($2^{10} \times 50$) that enables efficient digital processing and clean division from the internal hardware timebase of the National Instruments data acquisition system. This provides sufficient temporal resolution to capture both transient and steady-state torque behavior during tapping. Each acquisition was conducted for a duration sufficient to ensure that the complete tapping process, including engagement, steady cutting, and disengagement, was fully recorded.

The voltage signal was acquired in foreground mode, ensuring synchronized and uninterrupted data capture throughout the experiment.

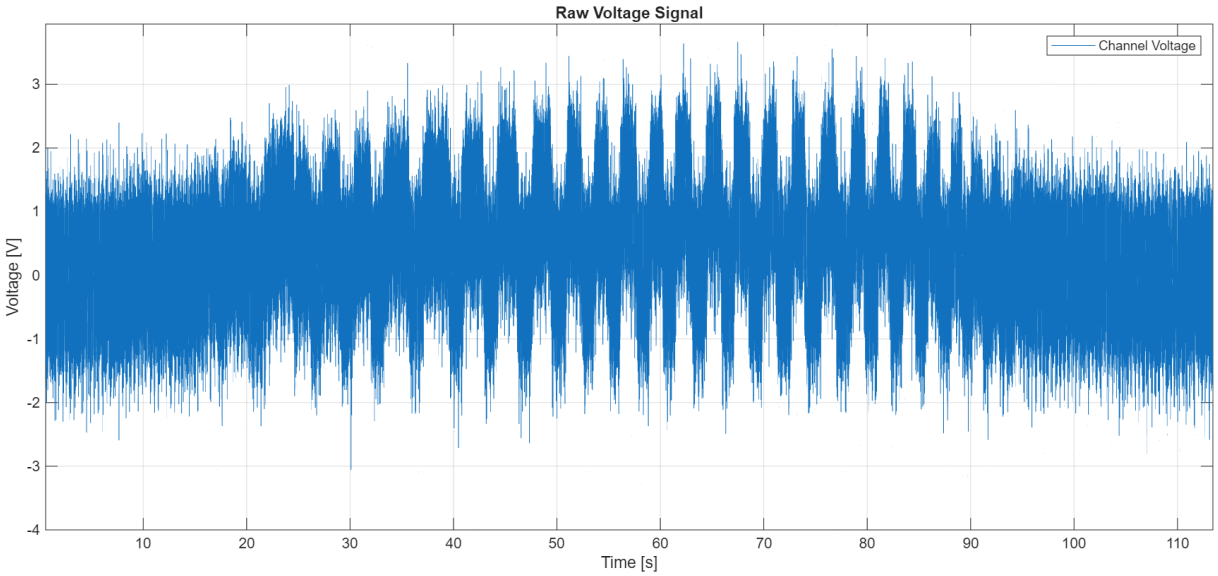

Figure 3.12: Raw voltage signal - acquired during experimental tapping operation

3.2.6. Signal Processing and Torque Evaluation

The raw voltage signal from the torque measurement system contained high-frequency noise originating from electronic components and environmental disturbances. To obtain a reliable torque signal, a structured signal processing procedure was implemented in MATLAB.

Noise Reduction

A median filter was applied to the zeroed voltage signal to remove impulsive noise and occasional electrical spikes. Median filtering effectively suppresses outliers while preserving the overall shape of the torque signal.

A fourth-order low-pass Butterworth filter was then applied to eliminate high-frequency noise components. A cutoff frequency of 500 Hz was selected based on the dynamic characteristics of the manual tapping process. Zero-phase filtering was used to prevent phase distortion of the signal.

In the figure 3.13, each distinct peak in the signal corresponds to a single manual lever action, representing half a revolution during the manual tapping operation.

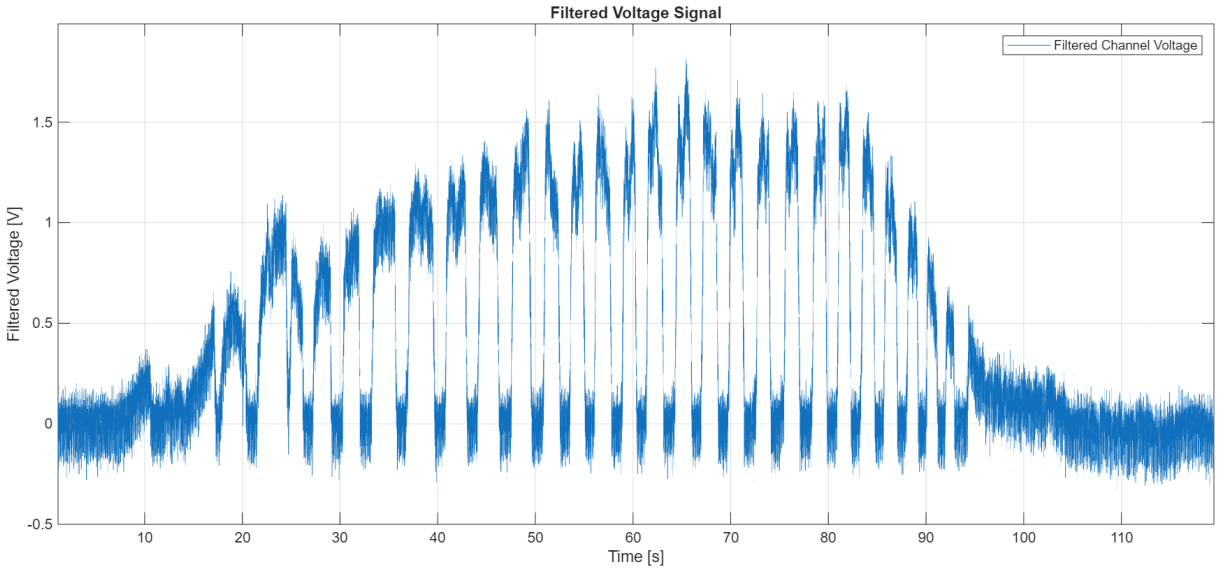

Figure 3.13: Filtered voltage - Filtered from Raw voltage using filter

Voltage-to-Torque Conversion

After filtering, the voltage signal was converted to torque using the calibration factor for the torque sensor and charge amplifier combination. A linear conversion factor of 4 N·m per volt was applied, yielding the torque signal as a function of time.

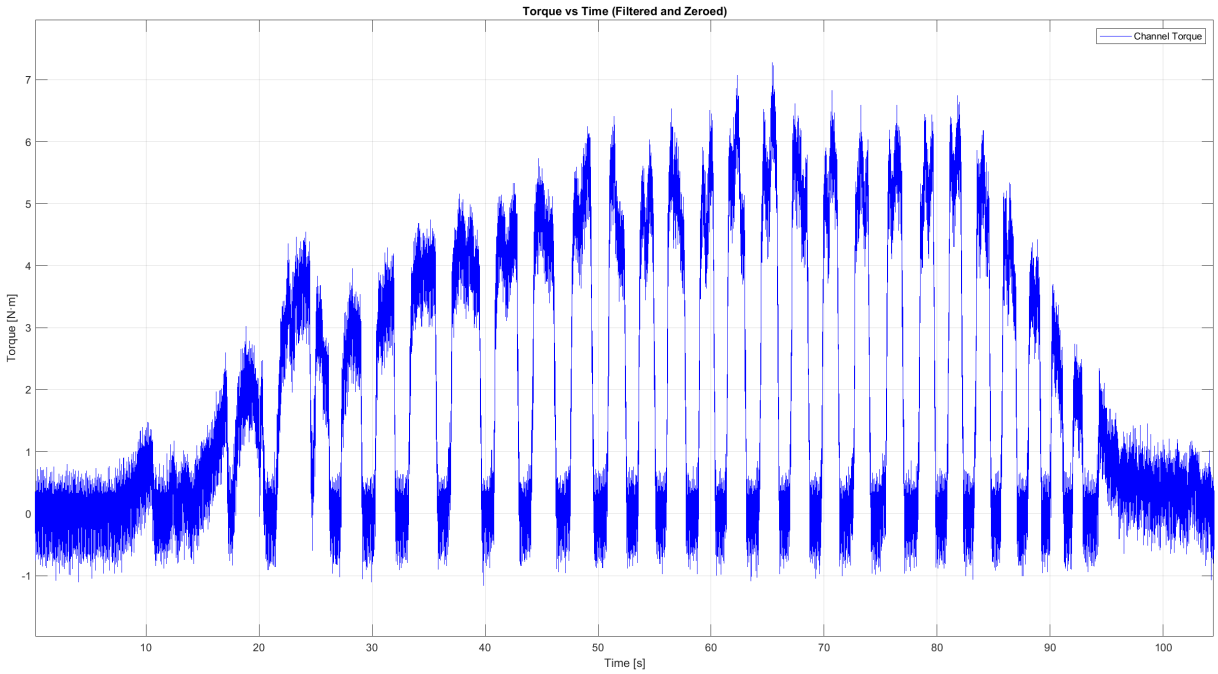

Figure 3.14: Torque - Converted from voltage signal

3.2.7. Experimental Procedure for Manual Tapping Tests

Manual tapping experiments were conducted using a consistent and repeatable procedure to ensure the reliability of the measured torque data. The procedure included the following steps:

1. The C45 steel workpiece, prepared with a pre-drilled central hole of the appropriate diameter, was rigidly mounted onto the torque sensor.
2. The torque sensor was securely fixed to the machine table to prevent any movement during tapping.
3. The data acquisition system was initialized, and torque recording was started prior to tool engagement.
4. Manual tapping was performed by applying a controlled rotational input to the tap until full thread engagement was achieved.
5. Torque data were continuously recorded throughout the tapping process.
6. After tapping was completed, data acquisition was stopped, and the recorded data were saved for post-processing.

Uniform tapping speed and consistent cutting conditions were maintained during each experiment. Multiple trials were conducted for each tap size and chamfer geometry to ensure repeatability.

The resulting torque data provided a reliable experimental basis for validating the analytical tapping torque model developed in the preceding Chapter 2.

3.2.8. Summary

This chapter described the experimental methodology used for both model calibration and validation. Orthogonal cutting experiments were conducted to identify cutting and edge force coefficients required for the mechanistic torque model. Independent tapping experiments were subsequently performed using a high-precision torque measurement system to validate the analytical predictions.

The clear separation between calibration and validation experiments enhances the reliability of the study and provides a robust framework for comparing analytical and experimental tapping torque results, which are discussed in the following chapter.

4 | Results and Discussion

4.1. Overview

This chapter presents the results of the analytical tapping torque model developed in Chapter 2 and the experimental investigations described in Chapter 3. The primary objective is to evaluate the predictive capability of the analytical model by comparing predicted tapping torque with experimentally measured torque values under identical cutting conditions.

The analytical model incorporates detailed tap geometry parameters, such as pitch, nominal diameter, pre-drill hole diameter, chamfer angle, chamfer length, calibration length, thread profile angle, rake angle, and cutting force coefficients obtained from orthogonal cutting experiments. Experimentally measured torque was obtained through manual tapping tests using identical tap geometries and workpiece material.

A comparative analysis was conducted to assess the agreement between analytical predictions and experimental measurements, as well as to identify sources of deviation between the two approaches.

4.2. Analytical Prediction of Tapping Torque

Analytical tapping torque was computed using the mechanistic force-based model developed in this study. For each tap geometry, the following input parameters were used:

1. Tap geometric parameters (pitch, nominal diameter, chamfer angle, chamfer length, calibration length)
2. Pre-drill hole diameter
3. Cutting and edge force coefficients obtained from orthogonal cutting calibration tests
4. Thread helix angle and tool rake geometry

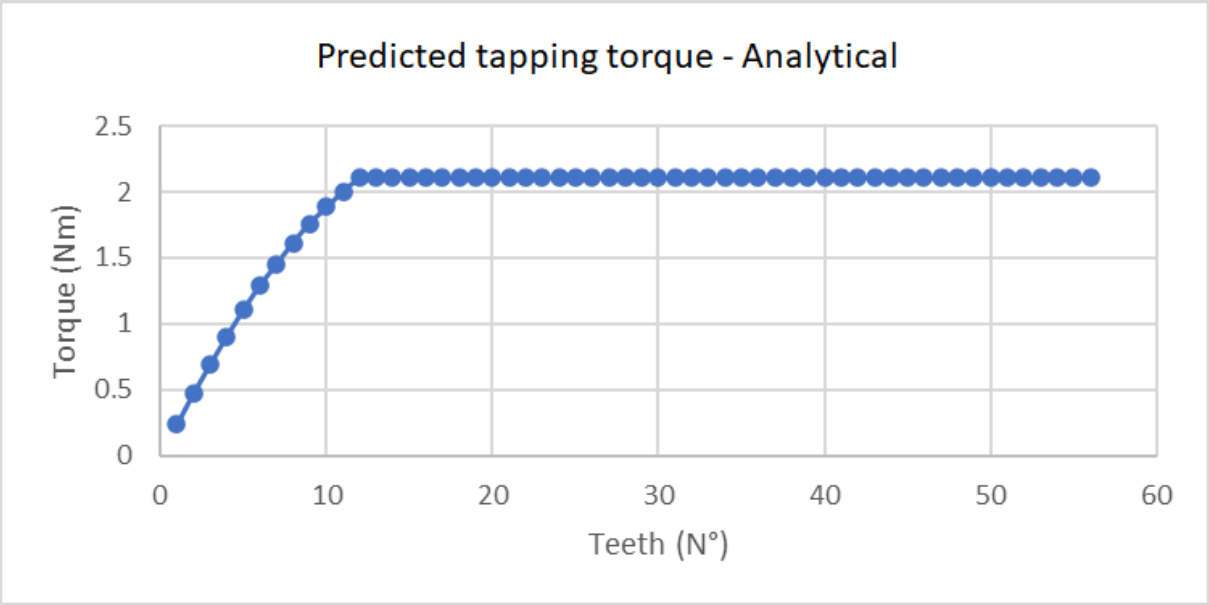

Figure 4.1: Result derived from Analytical model (M5x0.8)

As the tap enters the pre-drilled hole, an increasing number of cutting edges become active along the chamfer section, resulting in a gradual increase in torque.

Once the full chamfer is engaged, the torque reaches a saturation region in which both the cutting and calibration sections contribute to the total torque. In this region, the number of engaged cutting edges remains constant, and the torque stabilizes at its maximum value.

The analytical torque profile therefore consists of:

1. An initial torque rise during chamfer engagement
2. A saturated torque region corresponding to full thread formation

The maximum saturated torque predicted by the analytical model was extracted for quantitative comparison with the experimental results.

4.3. Experimental Measurement of Tapping Torque Evolution

The experimentally measured tapping torque exhibited a profile consistent with the physical stages of the tapping process.

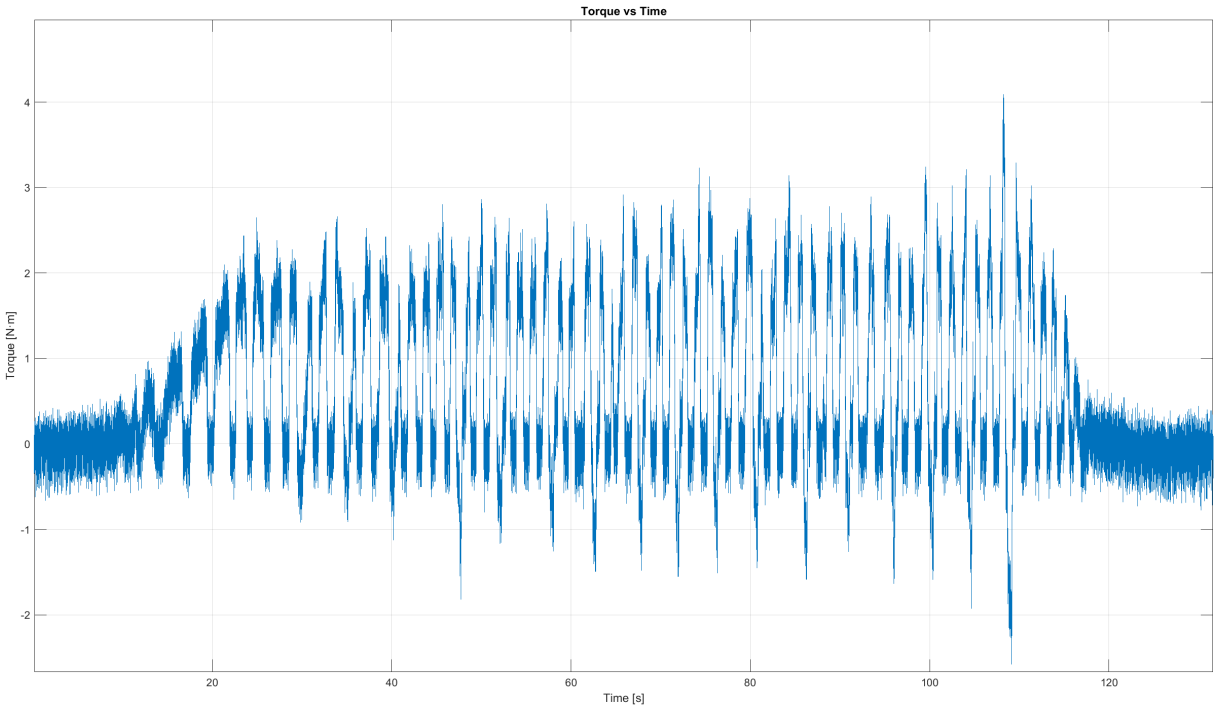

Figure 4.2: Experimental result (M5x0.8)

The acquired torque signal demonstrated the following characteristics:

1. Initial torque increase as the chamfered cutting edges progressively engaged with the workpiece
2. Torque saturation when the cutting and calibration sections were fully engaged
3. Torque reduction during tap withdrawal and disengagement

The experimental torque–time response was analyzed in its entirety. For direct comparison with the analytical model, the maximum saturated torque observed during full engagement was identified and used as the representative experimental torque value.

4.4. Comparison Between Analytical and Experimental Torque Profiles

Table 4.1: Comparison of Analytical and Experimental Torque for Tested Taps

Tested taps	Analytical torque (Nm)	Experimental (Nm)	% difference
M5	2.1	2.8	33 %
M6	4.6	5.4	17 %
M6	4.6	5.8	26 %
M8	5.4	7.2	33 %
M8	5.4	7	30 %
M10	8.75	12	37 %
M10	8.75	12.8	46 %
M12	12.5	14.2	14 %

A direct comparison between analytically predicted and experimentally measured torque values was performed for all tested tap sizes and geometries. Overall, the analytical model demonstrated good agreement 4.1 with the experimental results across the investigated range of tap diameters and chamfer configurations.

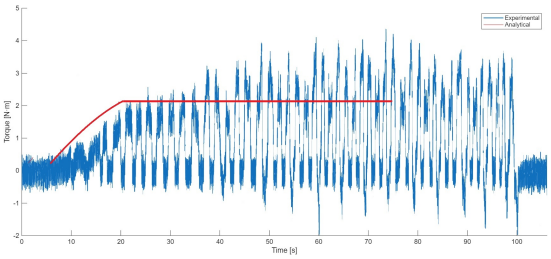

(a) M5 - Replica 1

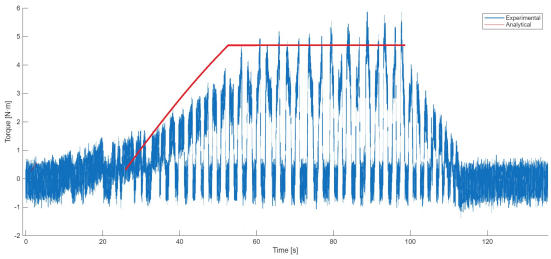

(b) M6 - Replica 1

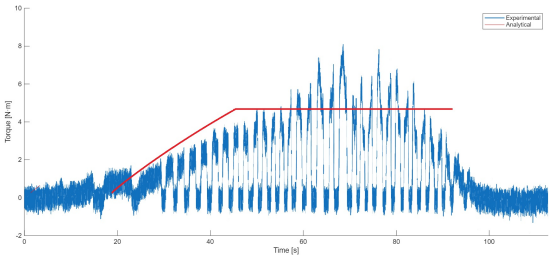

(c) M6 - Replica 2

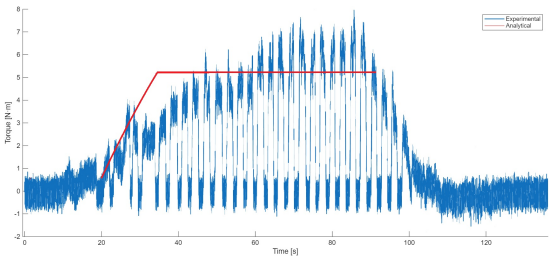

(d) M8 - Replica 1

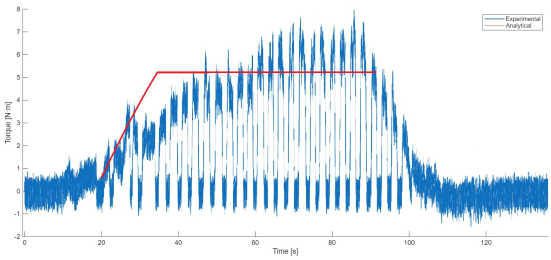

(e) M8 - Replica 2

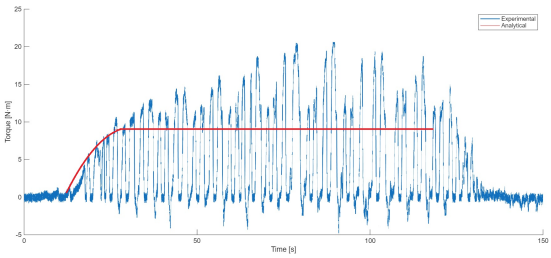

(f) M10 - Replica 1

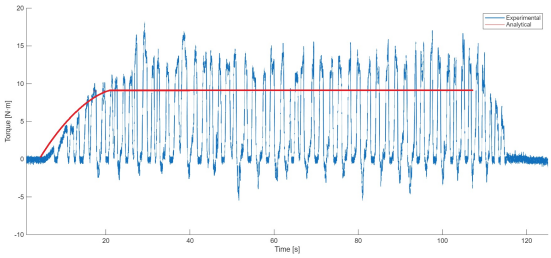

(g) M10 - Replica 2

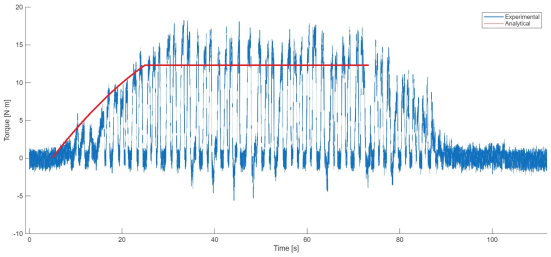

(h) M12 - Replica 1

Figure 4.3: Analytical vs Experimental tapping torque result analysis

The predicted torque values closely followed the experimental trends, accurately capturing the influence of tap size, pitch, and chamfer geometry on torque development. The difference between analytical and experimental torque values was within a few percentage points, indicating that the proposed model can reliably predict tapping torque under practical conditions.

In most cases, the analytical model slightly underestimated the experimentally measured torque. This outcome aligns with expectations, as the analytical formulation primarily accounts for cutting forces and assumes idealized friction conditions.

4.5. Discussion of Deviations Between Analytical and Experimental Torque

Although the analytical model demonstrated good agreement with experimental torque measurements, minor deviations were observed between predicted and measured saturated torque values.

- One contributing factor is the simplified force coefficient identification procedure. In this study, only the tangential force was measured during orthogonal cutting due to limitations in extracting feed force data from the CNC system. In a complete mechanistic formulation, both tangential and feed force components are required to accurately determine cutting and edge coefficients before transforming them into oblique coefficients. The absence of feed force measurement may introduce slight inaccuracies in the oblique force coefficients used for tapping torque prediction.
- Another source of deviation arises from friction effects during tapping. The analytical model assumes constant friction conditions along the cutting and calibration sections. In practice, friction varies due to chip packing, lubrication conditions, surface finish, and local temperature variations. These effects are difficult to model precisely and can increase or decrease the measured torque relative to theoretical predictions.
- Furthermore, manual tapping introduces non-uniform rotational speed and axial force fluctuations. Unlike rigid machine tapping, manual operation results in small variations in torque application and engagement consistency, contributing to experimental variability.

Despite these factors, the deviation between analytical and experimental saturated torque values remained relatively small, indicating that the developed model captures the dom-

inant mechanics governing tapping torque generation. These results confirm that the approach is fundamentally sound and identify areas for refinement in future studies.

4.6. Significance of Torque Saturation for Tool Design

The saturated torque region represents the maximum torque demand experienced by the tap during operation and is therefore the most critical parameter for tool design and failure prevention. Accurate prediction of this torque is essential for determining the optimal core diameter and ensuring adequate torsional strength of the tap.

The analytical model's ability to predict saturated torque with high accuracy provides a reliable foundation for the tap strength and optimization analysis presented in the subsequent chapter.

4.7. Summary

The main findings of this chapter can be summarized as follows:

- The analytical tapping torque model successfully predicts torque trends for various tap sizes and geometries.
- Experimental torque measurements show good agreement with analytical predictions, with deviations limited to a few percent.
- Differences between analytical and experimental results are primarily attributed to frictional effects, orthogonal-to-oblique force transformation, and manual tapping variability.
- The proposed model demonstrates strong potential for application in tap design optimization and failure prevention.

5 | Optimal Tap Core Diameter Analysis

Tap failure during tapping operations is primarily caused by torsional overload. An insufficient tap core diameter may result in premature failure under relatively low torque, whereas an excessively large core diameter reduces chip evacuation space, increasing the risk of chip packing and tap jamming. In these circumstances, additional torque is required to release the tap, which substantially raises the probability of torsional fracture.

Figure 5.1: Tapping tool torsional failure

Determining an optimal tap core diameter is essential to ensure adequate torsional strength while maintaining sufficient space for chip evacuation. This chapter introduces a combined analytical and experimental methodology for establishing the optimal core diameter of tapping tools, considering predicted tapping torque, material strength, stress concentration effects, and safety factors.

5.1. Analytical Framework for Tap Core Diameter Determination

5.1.1. Torsional Strength Criterion for Tapping Tools

The torsional strength of a tap depends on the maximum shear stress developed in its core under applied torque. For a circular shaft subjected to torsion, the relationship between applied torque and shear stress is described by the classical torsional formula.

In tapping operations, the analytically predicted maximum torque required for thread formation, as detailed in Chapter 2, represents the nominal operational torque. However, actual tapping conditions introduce additional uncertainties, including chip packing, frictional variation, and localized overloads.

To address these factors, the predicted tapping torque is multiplied by the following parameters:

- A safety factor, also referred to as the chip packing index, typically ranging from 3 to 4
- A stress concentration factor (SCF) that accounts for geometric discontinuities in the tap
- The material shear strength of the tap

These parameters enable calculation of the minimum core diameter required to safely withstand the applied torque.

5.1.2. Material Strength Consideration

The tapping tools examined in this study were manufactured from M35 high-speed steel (HSS). Supplier specifications indicate that the ultimate tensile strength (Rm) of this material is approximately 2900 MPa.

For torsional loading, following the Von Mises criterion, the maximum shear stress was conservatively estimated as 60% of the ultimate tensile strength, resulting in the following shear strength value:

$$\tau_{\text{material}} = 0.6 \times 2900 = 1740 \text{ MPa}$$

This value was used as the allowable shear stress in analytical determination of core diameter.

5.2. Experimental Verification of Material Shear Strength

To validate the assumed shear strength, a torsional test was performed on a solid cylindrical shaft made from the same M35 HSS material and heat-treated to match the hardness of the taps.

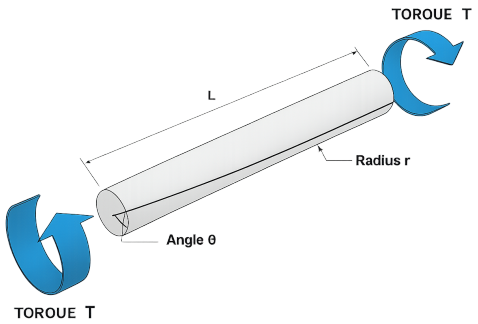

Figure 5.2: Torsional test illustration

$$\tau = \frac{T * r}{J} \tag{5.1}$$

where

- τ is the torsional shear stress (MPa or N/mm^2),
- T is the applied torque (N·mm),
- r is the radial distance from the center (mm),
- J is the polar moment of inertia of the cross-section (mm^4).

$$J = \frac{\pi r^4}{2}. \tag{5.2}$$

A 3.7 mm diameter shaft was subjected to torsional loading until fracture, failing at applied torques of 16.94 Nm, 17.1 Nm, and 17.06 Nm. Substituting these values into the torsional equation produced an average shear stress of approximately 1713.503 MPa, closely aligning with the value from material specifications.

Failure Torque (N·m)	Shear Stress (MPa)
16.94	1704.1
17.10	1720.2
17.06	1716.1

Table 5.1: Torsional Test Results for M35 HSS solid shaft (Diameter = 3.7 mm)

This experimental result confirmed the validity of the assumed material shear strength, supporting its use in subsequent analytical calculations.

5.3. Experimental Determination of Stress Concentration Factor

5.3.1. Need for Stress Concentration Factor

Unlike a uniform cylindrical shaft, a tap incorporates geometric features such as flutes, thread profiles, and chamfer transitions, which introduce stress concentrations. These features substantially increase local shear stress relative to an ideal solid shaft.

Accordingly, a stress concentration factor (SCF) is required to accurately represent the torsional behavior of the tap.

5.3.2. Torsional Failure Tests on Taps

To experimentally determine the stress concentration factor, tapping experiments were conducted using taps of sizes M5, M6, and M8, all manufactured from M35 HSS with identical hardness.

The tests were conducted in blind holes, ensuring that the taps reached the bottom of the hole and became mechanically constrained. Continued application of torque led to torsional failure, and the torque at failure was recorded for each tap size.

The core diameters of the failed taps were measured, and the torsional formula was applied to compute the apparent shear stress at failure for each tap. The resulting shear stress values were significantly higher than the material shear strength, indicating the influence of stress concentration effects.

Taps	Core Dia (mm)	Breaking Torque (N·m)	Shear Stress (N/mm^2)
M5	1.8	7.58	6622.8
M6	3.2	38.09	5923.1
M8	3.4	48.00	6222.9

Table 5.2: Breaking torque and shear stress for different tap sizes

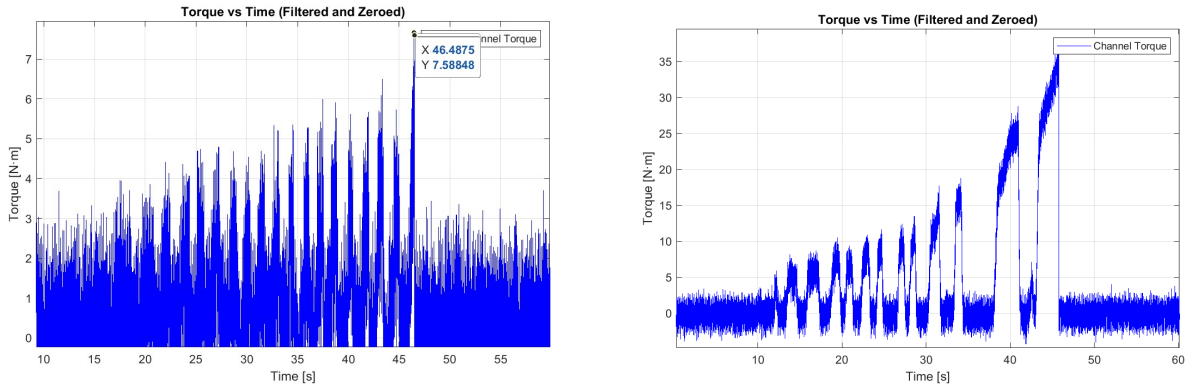

(a) a) M5 (b) b) M6

Figure 5.3: Tap breakage analysis

5.3.3. Evaluation of Stress Concentration Factor

The stress concentration factor was determined as the ratio of the apparent shear stress at tap failure to the material shear strength obtained from the torsional solid shaft test (1713.503 MPa).

For the tested taps, the average calculated stress concentration factor was approximately 3.65. This value was adopted as the representative SCF for M35 HSS taps with similar geometry.

5.4. Determination of Optimal Tap Core Diameter

Using the following parameters:

1. Predicted maximum tapping torque obtained from the analytical torque model
2. Safety factor (chip packing index) accounting for abnormal loading conditions
3. Stress concentration factor experimentally determined for the tap geometry
4. Allowable material shear stress validated through torsional testing

The minimum core diameter required to safely withstand the applied torque can then be calculated.

$$d_{c,\text{opt}} = \left(\frac{16\, T\, S_f\, K_t}{\pi\, \tau_{\text{material}}} \right)^{\frac{1}{3}} \tag{5.3}$$

where

- $d_{c,\text{opt}}$: Optimal core diameter of the tap (mm)
- T: Maximum tapping torque predicted analytically (N·mm)
- S_f : Safety factor / chip packing index
- K_t : Stress concentration factor
- τ_{material} :Allowable shear stress of tap material (MPa)

The resulting value represents the optimal core diameter, defined as the minimum diameter that ensures torsional integrity of the tap while providing adequate chip evacuation space.

Manufacturing taps with core diameters below this value significantly increases the risk of torsional failure. Conversely, larger core diameters reduce flute volume and may promote chip clogging, which indirectly increases torque and failure risk.

5.5. Summary

The principal outcomes of this chapter are summarized as follows:

- The analytically predicted maximum tapping torque provides a reliable basis for assessing tap strength.
- The shear strength of M35 HSS was experimentally verified to be approximately 1713.503 MPa.
- Stress concentration effects have a significant impact on tap torsional strength, with an experimentally determined stress concentration factor of 3.65.
- An optimal tap core diameter can be determined by integrating torque prediction, safety factor, stress concentration factor and material strength.
- The proposed methodology facilitates the design of failure-resistant taps without compromising chip evacuation capability.

6 | Conclusions and Future Work

6.1. Conclusions

This study developed and validated a mechanistic methodology to predict tapping torque and determine the minimum safe core diameter of a tapping tool using cutting mechanics and torsional strength analysis.

Orthogonal cutting experiments were conducted to determine the tool–workpiece force coefficients. Tangential cutting and edge coefficients were extracted from steady-state cutting data through linear regression of cutting force versus uncut chip thickness. These coefficients were subsequently converted into oblique cutting coefficients and integrated into the tapping torque prediction model.

By combining tap geometry parameters (pitch, nominal diameter, chamfer geometry, and calibration length) with the identified force coefficients, the analytical model predicted the torque evolution during tapping. The model accurately reproduced the physical stages of tapping, including initial chamfer engagement, torque increase during thread formation, and torque saturation resulting from full contact in the cutting and calibration regions.

Manual tapping experiments were performed using an instrumented torque measurement system. The measured torque profile exhibited the same characteristic behavior as predicted by the analytical model. Comparison of predicted and measured saturated torque values showed good agreement, with only minor percentage deviations. The residual discrepancies are mainly attributed to variations in friction, chip evacuation conditions, and the non-uniform loading associated with manual tapping.

The predicted torque was subsequently used to determine the minimum safe core diameter through torsional strength analysis. The shear strength of the tap material (M35 HSS) was experimentally validated via torsional testing of a blank specimen, closely matching the theoretical value. The stress concentration factor was established experimentally by controlled fracture of taps in blind holes, yielding an average value of 3.65.

By integrating predicted tapping torque, chip-packing safety factor, experimental stress

concentration factor and validated material shear strength, the minimum core diameter to prevent torsional failure during tapping can be calculated. This physics-based method improves tap design accuracy and reduces reliance on empirical standards.

During orthogonal cutting experiments, only the tangential cutting force was measured, as the CNC lathe controller provided only spindle torque data and not feed force. Consequently, the cutting and edge coefficients were identified using tangential force alone and subsequently converted into oblique coefficients. Despite this limitation, the predicted tapping torque closely matched experimental measurements, demonstrating the robustness of the proposed methodology.

6.2. Future Work

While the proposed model demonstrated strong predictive capability, several enhancements could further improve its applicability and industrial relevance.

- **Improved Force Coefficient Identification:** In this study, cutting and edge coefficients were identified using only tangential force from CNC spindle torque data, while the feed force could not be measured. A comprehensive mechanistic formulation requires both tangential and feed forces to accurately determine orthogonal cutting coefficients prior to conversion into oblique coefficients. Future research should utilize a dynamometer-based measurement system capable of simultaneously recording tangential and feed forces to enhance the accuracy of the tapping torque prediction model. (refer Appendix B)
- **Inclusion of friction modeling:** The current model assumes constant friction conditions. Incorporating a variable friction coefficient that accounts for lubrication, temperature, and cutting speed would enhance prediction accuracy.
- **Machine tapping validation:** This study employed manual tapping. Extending experiments to CNC or rigid tapping conditions would eliminate operator variability and facilitate dynamic torque modelling.
- **Different materials and coatings:** Future research should validate the model for difficult-to-cut materials, including stainless steel, titanium alloys, and coated taps, to broaden the methodology's applicability.

In summary, the presented approach establishes a foundation for predictive tap design and intelligent tapping process planning, bridging the gap between cutting mechanics and practical tooling selection.

Bibliography

[1] Y. Altintas. *Manufacturing Automation: Metal Cutting Mechanics, Machine Tool Vibrations, and CNC Design.* Cambridge University Press, Cambridge, UK, 2nd edition, 2012. ISBN 978-1-107-00148-0.

[2] E. Armarego and M. N. Chen. Predictive cutting models for the forces and torque in machine tapping with straight flute taps. *Annals of the CIRP*, Inferred, Inferred.

[3] T. C. Bera, H. Manikandan, A. Bansal, and D. Nema. A method to determine cutting force coefficients in turning using mechanistic approach. *International Journal of Materials Mechanics and Manufacturing.*

[4] S. Bhowmick, M. Lukitsch, and A. Alpas. Tapping of al–si alloys with diamond-like carbon coated tools and minimum quantity lubrication. *Journal of Materials Processing Technology*, 210:2142–2153, 2010.

[5] M. Bodden, C. Morgan Calhoun, M. Cohen, D. Lum, M. KaJuana, S. Toellner, and D. Dickel. Failure analysis of a m7x1 high-speed steel tap. *J Fail. Anal. and Preven.*, 22:1431–1441, 2022.

[6] T. Cao and J. W. Sutherland. Investigation of thread tapping load characteristics through mechanistics modeling and experimentation. *International Journal of Machine Tools & Manufacture*, 42:1527–1538, 2002.

[7] N. Chen and A. Smith. Modelling of machine tapping with straight flute taps. *Annals of the CIRP*, Inferred, Inferred.

[8] T. DEMİREL, S. YAĞMUR, Y. KAYIR, and A. KURT. Investigation of thrust force, torque and chip formation in tapping threading by finite element method. *POLİTEKNİK DERGİSİ / Journal of Polytechnic*, 27:1633–1641, 2024.

[9] A. P. S. Dogra, S. G. Kapoor, and R. E. DeVor. Mechanistic model for tapping process with emphasis on process faults and hole geometry. *Journal of Manufacturing Science and Engineering*, 124, 2002.

[10] F. Geßner, M. Weigold, and E. Abele. Measuring and modelling of process forces

during tapping using single tooth analogy process. *Production Engineering*, 15:97–107, 2021.

[11] D. Hajdu, A. Astarloa, I. Kovacs, and Z. Dombovari. The curved uncut chip thickness model: A general geometric model for mechanistic cutting force predictions. *International Journal of Machine Tools & Manufacture*, 188:104019, 2023.

[12] W. E. Henderer. On the mechanics of tapping by cutting. *Trans. ASME Journal of Engineering for Industry.* Paper No. 76-WA/Prod-25.

[13] T.-T. Le, H. T. Pham, H. K. Doan, and P. G. Asteris. Experimental and computational investigation of the effect of machining parameters on the turning process of c45 steel. *Advances in Mechanical Engineering*, 17(2):1–13, 2025. doi: 10.1177/16878132251318170.

[14] P. Lee and Y. Altintaş. Prediction od ball-end milling forces from orthogonal cutting data. *International Journal of Machine Tools and Manufacture*, 36, 1996.

[15] S. K. E. Lenz. Investigation in tool life of twist drills. *Annals of the CIRP*, 29, 1980.

[16] G. Lorenz. On tapping torque and tap geometry. *Annals of the CIRP*, 29, 1980.

[17] A. Markopoulos, N. Karkalos, N. Vaxevanidis, and D. Manolakos. Friction in orthogonal cutting finite elements models with large negative rake angle. *Tribology in Industry*, 38:214–220, 06 2016.

[18] T. D. Marusich. Effects of friction and cutting speed on cutting force. In *Proceedings of ASME Congress 2001*, New York, NY, November 2001.

[19] L. Meier, L. Seeholzer, and K. Wegener. A generalized force and chip flow model for oblique cutting and varying undeformed chip cross sections. *MM Science Journal*, Inferred, 2019.

[20] P. Monka, K. Monkova, V. Modrak, S. Hrica, and P. Pastucha. Study of a tap failure at the internal threads machining. *Engineering Failure Analysis*, 100:25–36, 2019.

[21] E. Oezkaya and D. Biermann. Segmented and mathematical model for 3d fem tapping simulation to predict the relative torque before tool production. *International Journal of Mechanical Sciences*, 128-129:695–708, 2017. doi: 10.1016/j.ijmecsci.2017.04.011.

[22] E. Oezkaya and D. Biermann. Development of a geometrical torque prediction method (gtpm) to automatically determine the relative torque for different tapping tools and diameters. *International Journal of Advanced Manufacturing Technology*, 97:1465–1479, 2018.

[23] I. C. Pereira, P. I. Vianello, D. Boing, G. Guimarães, and M. B. da Silva. An approach to torque and temperature thread by thread on tapping. *The International Journal of Advanced Manufacturing Technology*, 106:4891–4901, 2020.

[24] A. Popov and A. Dugin. Effect of uncut chip thickness on the ploughing force in orthogonal cutting. *International Journal of Advanced Manufacturing Technology*, 76:1937–1945, 2015.

[25] M. Popovic, L. Tanovic, and K. F. Ehmann. Cutting Forces Prediction the Experimental Identification of Orthogonal Cutting Coefficients. *University of Belgrade Faculty of Mechanical Engineering, Production Engineering Department*, Inferred.

[26] M. Popović, A. Stoić, and L. Tanović. Prediction of tapping forces and torque for 16mncr5 alloyed steel. *Tehnicki vjesnik - Technical Gazette*, June 2016.

[27] R. Puzović and B. Kokotović. Prediction of thrust force and torque in tapping operations using computer simulation. *FME Transactions*, 34:1–5, 2006.

[28] Y. Saito, S. Takiguchi, T. Yamaguchi, K. Shibata, T. Kubo, W. Watanabe, S. Oyama, and K. Hokkirigawa. Effect of friction at chip–tool interface on chip geometry and chip snarling in tapping process. *International Journal of Machine Tools & Manufacture*, 107:60–65, 2016.

[29] M. Wan, Y.-C. Ma, J. Feng, and W.-H. Zhang. Mechanics of tapping process with emphasis on measurement of feed error and estimation of its induced indentation forces. *International Journal of Machine Tools & Manufacture*, 114:8–20, 2017.

A | Appendix A

A.1. Determination of Average Tangential Force from Orthogonal Cutting Tests

This appendix explains in detail how the average tangential cutting force was determined for each feed rate during the orthogonal turning experiments.

During each cutting test, the spindle torque signal was recorded directly from the CNC controller. The recorded torque was then converted into tangential cutting force using the known tool radius relationship 3.1.

For every selected feed rate, the force–time signal exhibited three distinct regions:

1. **Initial engagement region** – The force increased gradually as the cutting tool made contact with the workpiece and the depth of cut was fully established.
2. **Steady-state cutting region** – The force stabilized once the tool was fully engaged in the material and uniform chip formation occurred.
3. **Exit region** – The force decreased as the tool disengaged from the workpiece at the end of the cut.

Only the steady-state region was considered for force analysis. The transient portions at the beginning and end of the signal were excluded to avoid inaccuracies caused by partial engagement or disengagement.

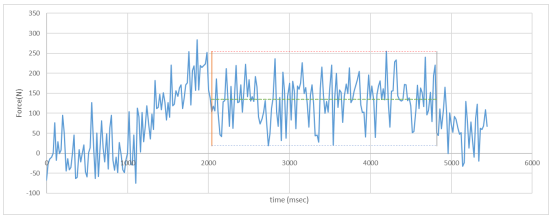

(a) Feed rate - 0.15mm (Replica 1)

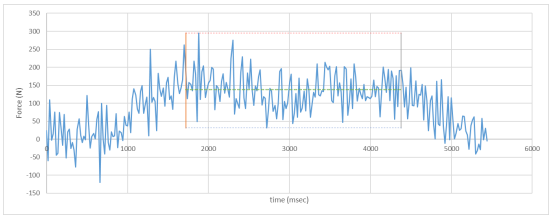

(b) Feed rate - 0.15mm (Replica 2)

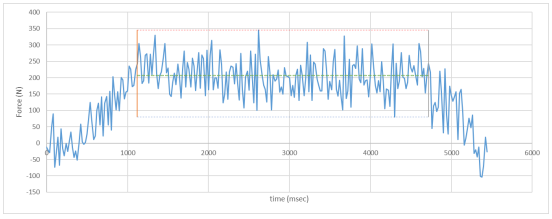

(c) Feed rate - 0.2mm (Replica 1)

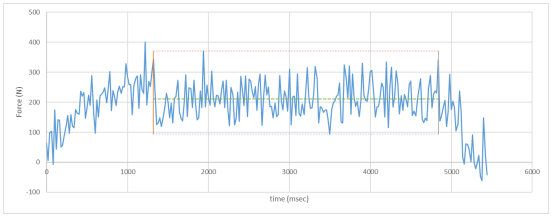

(d) Feed rate - 0.2mm (Replica 2)

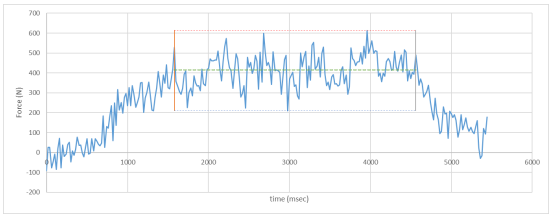

(e) Feed rate - 0.3mm (Replica 1)

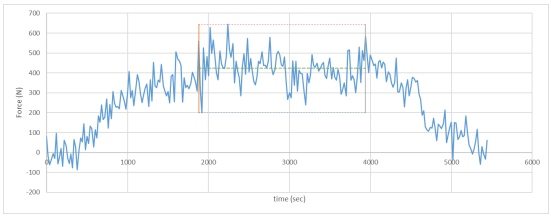

(f) Feed rate - 0.3mm (Replica 2)

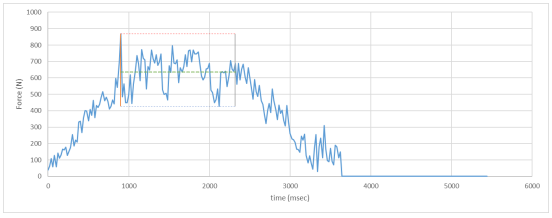

(g) Feed rate - 0.45mm (Replica 1)

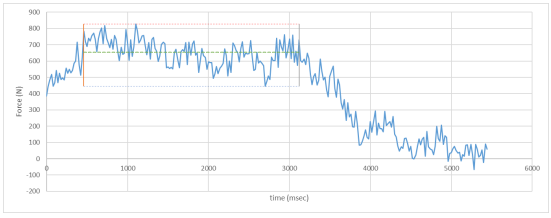

(h) Feed rate - 0.45mm (Replica 2)

Figure A.1: Force–time plots for each feed rate highlighting the selected steady-state region.

For each feed rate:

- The steady-state portion of the force–time graph was visually identified.
- A consistent time window within this region was selected.
- The average tangential force was calculated using the mean value of the selected steady-state samples.

The resulting average force values were tabulated against their corresponding feed rates and depth of cut.

Uncut chip thickness(mm)	Ft_Avg. (N)	Ft_Avg. (N)	Width of cut (mm) (b)	Ft/b
0.15 0.15	134.32 138.25	136.29	1.5	90.86
0.2 0.2	206.55 211.64	209.10		139.40
0.3 0.3	415.14 422.60	418.86		279.23
0.45 0.45	636.91 653.74	645.32		430.22

Table A.1: Average tangential force calculation for different uncut chip thickness values

These averaged values were then used to:

- Plot the relationship between tangential force and feed rate.
- Determine the cutting force coefficient and edge force coefficient using linear regression.

The graph 3.8 presented in the experimental chapter was generated from these averaged force values. This systematic averaging procedure ensured that only stable cutting data contributed to the force coefficient identification, thereby improving the reliability of the mechanistic model.

B | Appendix B

B.1. Improved Force Coefficient Identification

In the present study, the tangential cutting force was obtained from the spindle torque data available in the CNC controller. However, the feed force could not be measured due to limitations in accessing additional data from the machine system.

In conventional mechanistic modeling of cutting processes, both tangential and feed forces are required to accurately determine the cutting and edge force coefficients in orthogonal cutting. (2.13, 2.14, 2.15 and 2.16) These coefficients are then transformed into oblique cutting coefficients for use in tapping torque prediction models.

For future research, it is recommended to perform orthogonal cutting tests on a conventional lathe machine equipped with a multi-axis force dynamometer. Such a system would allow simultaneous measurement of i) Tangential cutting force and ii) Feed force

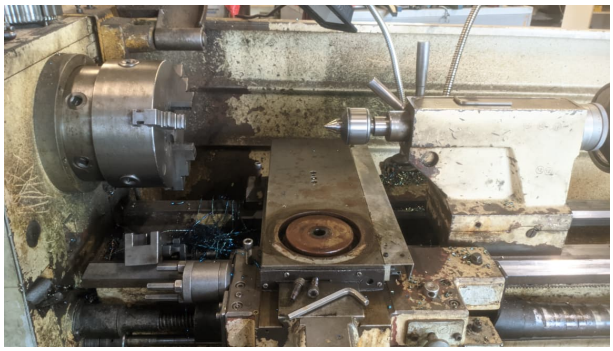

(a) Conventional Lathe

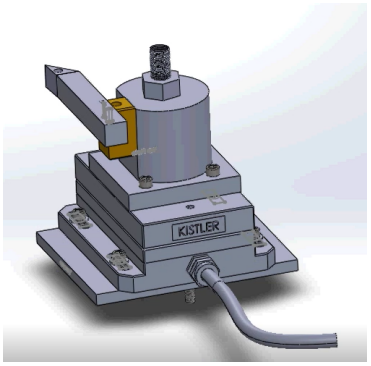

(b) 3D CAD design, Dynamometer positioning on Lathe

Figure B.1: Proposing Framework for Future Investigation

By measuring both tangential and feed forces, a full identification of orthogonal cutting coefficients can be carried out. This would lead to more precise oblique coefficient transformation and further improve the prediction accuracy of the tapping torque model.

List of Figures

List of Tables

List of Symbols/Nomenclature

Variable	Description	SI Unit
d	Nominal tap diameter	mm
d_c	Core diameter of tap	mm
d_p	Pre-drill hole diameter	mm
p	Thread pitch	mm
z	Number of flutes	–
β	Thread helix angle	°
γ	Rake angle	°
κ_c	Chamfer angle	°
a	Radial depth of cut in tapping	mm
i	Tooth index in tap	–
$x(i)$	Axial position of cutting edge	mm
$H(i)$	Chip thickness of respective cutting edge	mm
$A(i)$	Chip area of respective cutting edge	mm^2
$L(i)$	Contact length of respective cutting edge	mm
b'	Maximum Width of undeformed chip in tapping operation	mm
T	Tapping torque	N·m
r	Effective cutting radius	mm
h	Uncut chip thickness in orthogonal cutting test	mm
b	Width of cut in orthogonal cutting test	mm
F_i $(i = t, f, r)$	Tangential, Feed and Radial cutting force	N
dF_i $(i = t, f, r)$	Tangential, Feed and Radial discrete force	N
dF_{ic} $(i = t, f, r)$	Tangential, Feed and Radial discrete cutting force	N
dF_{ie} $(i = t, f, r)$	Tangential, Feed and Radial discrete edge force	N
K_{ic} $(i = t, f)$	Orthogonal cutting force coefficient (tangential/feed)	N/mm^2

K_{ie} $(i = t, f)$	Orthogonal edge force coefficient (tangential/feed)	N/mm
K'_{ic} $(i = t, f)$	Oblique converted cutting force coefficient (tangential/feed)	N/mm^2
K'_{ie} $(i = t, f)$	Oblique converted edge force coefficient (tangential/feed)	N/mm
$F_t(i)$	Tangential force component in i-th tooth	N
$F_r(i)$	Radial force component in i-th tooth	N
α	Thread profile angle	°
λ_s	Helix (oblique) angle in oblique cutting	°
η_c	Chip flow angle in oblique cutting	°
$d_{c,opt}$	Optical core diameter of tap	mm
$\tau_{material}$	Material shear strength	MPa
K_t	Stress concentration factor	–
SCF	Safety factor (chip packing index)	–
J	Polar moment of inertia	mm^4

Acknowledgements

First and foremost, I would like to express my sincere gratitude to **Professor Annoni Massimiliano Pietro Giovanni** academic supervisor for his constant guidance, valuable suggestions, and academic support throughout this project. His experience and constructive feedback played an essential role in shaping this work. I am also thankful to all his research assistants for their support and for generously sharing their knowledge. A special thanks goes to **Alessandro Tenconi** research assistant for his continuous assistance, technical discussions, and readiness to help whenever required.

This thesis was carried out in collaboration with organization **Boccassini srl, Gessate, Italy**. I sincerely thank the company for providing me with the opportunity to work on this industrial project and for making the necessary resources and facilities available. I am especially grateful to **Mr.Sergio Pietro** CEO at Boccassini srl for his trust and encouragement throughout the project. My heartfelt thanks also go to **Mr.Maurizio** technical mentor at Boccassini srl, for supporting me from the initial stages until the completion of this work. His practical guidance and constant availability were fundamental to the successful realization of this project.

I would also like to thank organization **WataJet srl, Italy** for supporting the orthogonal cutting experiments conducted as part of this research. Special thanks to **Mr.Luca Villa** staff at WataJet srl for his help in scheduling the experiments and ensuring they were completed on time. His cooperation and support were greatly appreciated.

Finally, I would like to thank my family and close friends for their continuous encouragement, patience, and belief in me throughout this journey. Their support has been a constant source of motivation during the completion of this thesis.

I am sincerely grateful to everyone who contributed to this work in any way.